Aus der Abteilung Neurophysiologie
(Leitung: Professor Dr. Ch. Fahlke)
des Zentrums Physiologie
der Medizinischen Hochschule Hannover

Der Anionenkanal des neuronalen Glutamattransporters EAAT4

Dissertation zur Erlangung des Doktorgrades der Medizin
in der Medizinischen Hochschule Hannover
vorgelegt von
Nico Melzer
aus Georgsmarienhütte

Hannover 2006

Angenommen vom Senat der Medizinischen Hochschule Hannover am 09.01.2007.

Gedruckt mit Genehmigung der Medizinischen Hochschule Hannover.
Präsident: Professor Dr. D. Bitter-Suermann

Betreuer: Professor Dr. Ch. Fahlke
Referent: Professor Dr. S. Papadopoulos
Korreferent: Priv.-Doz. Dr. K. Krampfl

Tag der mündlichen Prüfung: 09.01.2007
Promotionsausschußmitglieder: Professor Dr. K. D. Jürgens
Professor Dr. S. Lenzen
Professor Dr. T. Brinker

Meinen Eltern

Nico Melzer, Alexander Biela, Christoph Fahlke

Glutamate modifies ion conduction and voltage-dependent gating of excitatory amino acid transporter-associated anion channels

Journal of Biological Chemistry 2003

THE JOURNAL OF BIOLOGICAL CHEMISTRY
Vol. 278, No. 50, Issue of December 12, pp. 50112–50119, 2003
Printed in U.S.A.
© 2003 by The American Society for Biochemistry and Molecular Biology, Inc.

Glutamate Modifies Ion Conduction and Voltage-dependent Gating of Excitatory Amino Acid Transporter-associated Anion Channels*

Received for publication, July 23, 2003, and in revised form, September 18, 2003
Published, JBC Papers in Press, September 23, 2003, DOI 10.1074/jbc.M307990200

Nico Melzer‡, Alexander Biela‡, and Christoph Fahlke‡§¶

From the ‡Institute of Physiology, RWTH Aachen, 52057 Aachen, Germany and §Centro de Estudios Cientificos, Avenida Prat 514, Valdivia, Chile

Excitatory amino acid transporters (EAATs) mediate two distinct transport processes, a stoichiometrically coupled transport of glutamate, Na^+, K^+, and H^+, and a pore-mediated anion conductance. We studied the anion conductance associated with two mammalian EAAT isoforms, hEAAT2 and rEAAT4, using whole-cell patch clamp recording on transfected mammalian cells. Both isoforms exhibited constitutively active, multiply occupied anion pores that were functionally modified by various steps of the $Glu/Na^+/H^+/K^+$ transport cycle. Permeability and conductivity ratios were distinct for cells dialyzed with Na^+- or K^+-based internal solution, and application of external glutamate altered anion permeability ratios and the concentration dependence of the anion influx. EAAT4 but not EAAT2 anion channels displayed voltage-dependent gating that was modified by glutamate. These results are incompatible with the notion that glutamate only increases the open probability of the anion pore associated with glutamate transporters and demonstrate unique gating mechanisms of EAAT-associated anion channels.

Excitatory amino acid transporters (EAATs)[1] mediate the removal of glutamate from the synaptic cleft in the central nervous system and the uptake of glutamate in kidney and intestine (1–3). Five structurally distinct subtypes of mammalian glutamate transporters, EAAT1–EAAT5, have been identified in recent years (4–9). Each of these isoforms exhibits two separate transport processes: a stoichiometrically coupled cotransport of one glutamate with three Na^+ ions and one H^+, in countertransport to one K^+ ion (10, 11); and an anion conductance that appears to be pore-mediated. The EAAT-associated anion channel is currently thought to function as a glutamate-gated channel with a tight coupling of channel opening and closing to conformational changes of the corresponding carrier domain. In this model, only certain carrier conformations are associated with conducting anion pores, and the anion channel cycles between conducting and non-conducting states during transitions through various conformational states of the glutamate carrier (8, 9, 12–15).

We investigated anion conduction properties of two EAAT isoforms, human EAAT2 and rat EAAT4, using patch clamp recordings of transfected tsA201 cells under conditions that eliminate the $Glu/Na^+/H^+/K^+$ current component. Our results demonstrated that opening and closing of the EAAT-associated anion channels as well as the interaction with the glutamate uptake process are more complex than previously assumed. External glutamate modifies intrinsic properties of EAAT2- and EAAT4-associated anion channels such as anion selectivity and the rate constants of anion permeation. Moreover, EAAT4 anion channels exhibit voltage-dependent opening and closing transitions that are modified by glutamate. These results provide novel insights into the function of neurotransmitter transporters and illustrate similarities as well as differences between transporter-associated pores and ion channels.

EXPERIMENTAL PROCEDURES

Expression of hEAAT2 and rEAAT4 in tsA201 and HEK293 Cells—A pcDNA3.1-hEAAT2 construct was generated by subcloning the coding region of hEAAT2 (16) (kindly provided by Dr. M. Hediger, Harvard Medical School, Boston) into a pcDNA3.1 vector (Invitrogen) using flanking NotI restriction sites. The pcDNA3.1-rEAAT4 construct was kindly provided by Dr. J. Rothstein, The Johns Hopkins University, Baltimore (17). Transient transfection of tsA201 cells using the $Ca_3(PO_4)_2$ technique was performed as described previously (18). To identify cells with a high probability of expressing recombinant transporters, cells were cotransfected with a plasmid encoding the CD8 antigen and incubated 5 min before use with polystyrene microbeads precoated with anti-CD8 antibodies (Dynabeads M-450 CD8, Dynal, Great Neck, NY) (19). Only cells decorated with microbeads were used for electrophysiological recordings. By adjusting the CD8/EAAT cDNA ratio, we optimized our conditions so that almost every cell with beads exhibited a current component with characteristic properties shown in Fig. 1. For each construct, two independent recombinants were examined and exhibited indistinguishable functional properties. Oligoclonal cell lines stably expressing hEAAT2 were obtained by selection for resistance to the aminoglycoside antibiotic geneticin (G418, Roche Applied Science) as described previously (18). The stable cell lines so obtained exhibited electrical properties indistinguishable from transiently transfected tsA201 cells. Untransfected tsA201 cells displayed a negligible endogenous anion current component (current amplitude at −175 mV: Cl^-, −54 ± 6 pA; NO_3^-, −63 ± 13 pA; SCN^-, −56 ± 10 pA; at +125 mV: Cl^-, 40 ± 3 pA; NO_3^-, 31 ± 3 pA; SCN^-, 211 ± 13 pA, $n >$ 5 cells) that was not modified by the addition of glutamate.

Whole-cell Recordings—Standard whole-cell patch clamp recordings were performed using an Axopatch 200B (Axon Instruments, Union City, CA) or EPC10 (HEKA Electronics, Lambrecht, Germany) amplifier. Borosilicate pipettes were pulled with resistances of 1.0–2.2 megohms. More than 80% of the series resistance was compensated by an analog procedure resulting in calculated voltage errors <5 mV. Currents were filtered at 5 kHz and digitized with a sampling rate of 50 kHz using a Digidata (Axon Instruments) or an ITC-16 (HEKA) AD/DA converter. Cells were clamped to 0 mV for at least 2 s between test sweeps. The compositions of the standard solutions are as follows: extracellular (in mM) 140 NaCl, 4 KCl, 2 $CaCl_2$, 1 $MgCl_2$, 5 HEPES, pH 7.4; intracellular (in mM) 115 NaCl, 2 $MgCl_2$, 5 EGTA, 10 HEPES, pH 7.4. For certain experiments, NaCl in the intra- or extracellular solution was equimolarly substituted with $NaNO_3$, NaSCN, KCl, KNO_3, or KSCN. Substrate-containing external solutions were made by adding 0.5 mM L-glutamate. Anion currents were recorded always under con-

* This work was supported by the Deutsche Forschungsgemeinschaft Grant FOR450/1 (to C. F.). The costs of publication of this article were defrayed in part by the payment of page charges. This article must therefore be hereby marked "*advertisement*" in accordance with 18 U.S.C. Section 1734 solely to indicate this fact.

¶ To whom correspondence should be addressed: Institute of Physiology, RWTH Aachen, Pauwelsstr. 30, 52057 Aachen, Germany. Tel.: 49 241 80 88810; Fax: 49 241 80 82434; E-mail: chfahlke@physiology.rwth-aachen.de.

[1] The abbreviation used is: EAATs, excitatory amino acid transporters.

This paper is available on line at http://www.jbc.org

ditions that abolish stoichiometric glutamate current, *i.e.* in the absence of external glutamate or internal K^+ (20). For determination of anion permeability and conductivity ratios for external anions, cells were moved into the stream of solutions containing various sodium salts (in mM) 140 Na*X*, 4 KCl, 2 $CaCl_2$, 1 $MgCl_2$, 5 HEPES, pH 7.4 (*X* denotes Cl^-, I^-, NO_3^-, and SCN^-). To test for a concentration dependence of biionic reversal potentials (Fig. 4*C*), measurements were performed on cells internally dialyzed with (in mM) *X* $NaNO_3$, 117-*X* sodium gluconate, 5 EGTA, 10 HEPES, pH 7.4, in an external solution containing (in mM): *Y* NaSCN, 150-*Y* sodium gluconate, 5 HEPES, pH 7.4 (ratio *X*/*Y* = 117:150). For the experiments shown in Fig. 5, solutions with various external [SCN^-] were made by substituting NaSCN in the external standard solution with equimolar NaCl, as the Cl^- conductance of EAAT2 is negligible compared with SCN^- (Fig. 2). For all these experiments, we used external and/or internal agar salt bridges, made from a plastic tubing filled with 3 M KCl in 0.3% agar, to connect the Ag/AgCl electrode. Offset potentials determined at the end of each experiment, and junction potentials either calculated using the JPCalc software (Dr. P. Barry, University of South Wales, Sydney, Australia (21)) or directly measured (22) were used to correct results.

Data Analysis—Data were analyzed with a combination of pClamp (Axon Instruments, Union City, CA) and SigmaPlot (Jandel Scientific, San Rafael, CA) programs. Current amplitudes were used without subtraction procedure, and all summary data are shown as means ± S.E. For statistical evaluation the Student's *t* test was used.

To obtain current-voltage relationships in various internal or external anions, isochronal current amplitudes were determined 1 ms after the voltage step. Current ratios given in Fig. 4 were determined by dividing isochronal current amplitudes obtained from the same cell after application of 0.5 mM L-glutamate by the corresponding value before application of external substrate. For the determination of normalized current amplitudes as a mean of channel selectivity (Tables I and II), we divided current amplitudes in various external anions by the corresponding value determined from the same cell in a NO_3^--based external solution, rather than in a standard external solution to minimize errors introduced by dividing by the rather small current amplitudes of cells expressing EAAT2 in external Cl^-. Reversal potentials were only used for further analysis when the cell exhibited a whole-cell conductance that was at least three times larger than the mean value for untransfected cells under identical conditions. Permeability ratios were calculated from reversal potential measurements under biionic conditions using the Goldman-Hodgkin-Katz equation as described (18) (Tables I and II). Affinity constants (K_D) (Fig. 5) were calculated by plotting isochronal current amplitudes *versus* $[SCN^-]_e$ after a Lineweaver-Burk transformation and fitting a linear function with a least square routine with Excel (Microsoft) and Sigma Plot (Jandel Scientific). K_D values were determined from individual cells, in the absence and in the presence of L-glutamate, and all K_D values provided are means ± S.E. of 7 individual cells. The voltage dependence of the relative open probability (Fig. 7*A*) was determined by plotting the normalized instantaneous current amplitude at + 90 mV after 0.2-s prepulses to different voltages *versus* the preceding potential. Activation curves obtained in this manner were then fit with a single Boltzmann term plus a voltage-independent value ($I(V) = I_0/(1 + e^{V-V_{0.5}/kV}) + P_{min}$). To describe the time course of current inactivation, a sum of two exponentials and a time-independent value were fit to data recorded during a series of voltage steps from a holding potential of 0 mV (Fig. 7*B*). To describe the recovery from inactivation, we used a pulse protocol consisting of a 150-ms conditioning pulse to +160 mV, a hyperpolarizing prepulse (to potentials between −180 and −120 mV) of variable duration, and a fixed test step to +160 mV (Fig. 7*C*). The dependence of the peak current amplitude on the prepulse duration was fit with a single exponential giving the time constant of recovery from inactivation (Fig. 7*D*).

Noise Analysis—Non-stationary noise analysis (23, 24) was performed using an EPC10 amplifier (HEKA Electronics, Lambrecht, Germany) equipped with a 16-bit AD/DA converter as described (18). Currents were filtered at 10 kHz and digitized with a sampling rate of 50 kHz. Cells were held at the current reversal potential, and a series of 300 records was recorded by pulsing to a certain voltage. Pairs of subsequent records were then subtracted using the PulseTools software (HEKA Electronics, Lambrecht, Germany) to compute the experimental non-stationary ensemble variance (25). The variance determined in cells expressing EAAT4 was significantly larger than the background noise observed in non-transfected cells, and we observed a clear correlation between current and noise amplitudes determined at different cells. The amplitude of a current noise generated by the opening and closing of ion channels depends on the unitary current amplitude (*i*), the number of channels (*N*), and the absolute open probability (*P*) of the underlying channels (23, 24) as shown in Equation 1.

$$\sigma^2 = Ni^2P(1 - P) \quad \text{(Eq. 1)}$$

To determine the single channel amplitude at a certain potential, the background variance (σ_0^2) measured at the current reversal potential was subtracted from variances determined at various time periods after a voltage step to positive potentials (+120 to +160 mV). The subtracted variances were sorted into current bins (25) and plotted *versus* the corresponding mean current amplitude (Fig. 6). Under these experimental conditions the absolute open probability changes with time as given by Equation 2,

$$P(t) = \frac{I(t)}{iN} \quad \text{(Eq. 2)}$$

yielding Equation 3.

$$\sigma^2(t) - \sigma_0^2 = iI(t) - \frac{I^2(t)}{N} \quad \text{(Eq. 3)}$$

A fit of Equation 3 to the variance *versus* mean current (24) plot allowed us to determine the unitary current amplitude and the number of anion channels. By using these two values we calculated the absolute open probabilities (*P*) at the holding potential by extrapolating the instantaneous macroscopic current amplitude (I_{inst}) and dividing this amplitude by the number of channels (*N*) and the single channel amplitude (*i*) as shown in Equation 4.

$$P = \frac{I_{inst}}{Ni} \quad \text{(Eq. 4)}$$

RESULTS

EAAT-associated Anion Currents Are Active in the Absence of Transporter Substrate—Fig. 1 shows representative recordings from tsA201 cells expressing EAAT2 and EAAT4. Cells were intracellularly dialyzed with a potassium-free solution and extracellularly perfused with glutamate-free solutions with either Cl^- (Fig. 1, *A* and *D*), NO_3^- (Fig. 1, *B* and *E*), or SCN^- (Fig. 1, *C* and *F*) as main anions. These conditions eliminated the Glu/Na^+/H^+/K^+ current component (20) and allowed us to record anion currents in isolation. For cells expressing EAAT2, currents in external Cl^- were small (current amplitude at +125 mV: 0.11 ± 0.02 nA, $n = 16$) (Fig. 1*A*). Substitution of Cl^- by NO_3^- (Fig. 1*B*) or SCN^- (Fig. 1*C*) increased the anion influx at positive potentials and also the chloride efflux at negative potentials. Cl^- currents in cells expressing EAAT4 were larger than those in cells expressing EAAT2 (current amplitude at +125 mV: 0.27 ± 0.05 nA, $n = 12$) (Fig. 1*D*). Again, external NO_3^- (Fig. 1*E*) and SCN^- (Fig. 1*F*) enhanced the current amplitudes at negative and positive potentials as compared with recordings in external Cl^-. Under all external anion compositions EAAT2- and EAAT4-associated anion currents rose instantaneously upon voltage steps to negative and positive potentials. The two isoforms differed in the time course of current responses to depolarizing voltage steps. Whereas EAAT4-associated currents decayed in a voltage- and time-dependent manner, such current relaxations could not be observed in cells expressing EAAT2 (Fig. 1).

Fig. 2*A* shows the voltage dependence of the absolute EAAT2-associated current amplitudes for external Cl^-, I^-, NO_3^-, and SCN^- in the absence of external glutamate. EAAT2 displayed a SCN > NO_3 > I > Cl conductivity sequence (Table I). Fig. 2*B* presents averaged isochronal current amplitudes for cells intracellularly dialyzed with solutions containing Cl^-, NO_3^-, and SCN^- illustrating a higher conductivity also for intracellular polyatomic anions compared with Cl^- (Table II). Permeability ratios from the reversal potentials obtained in these experiments revealed for EAAT2 a relative anion permeability sequence of $P_I > P_{SCN} > P_{NO3} > P_{Cl}$ for external anions (Table I), and a $P_{SCN} > P_{NO3} > P_{Cl}$ sequence for internal anions

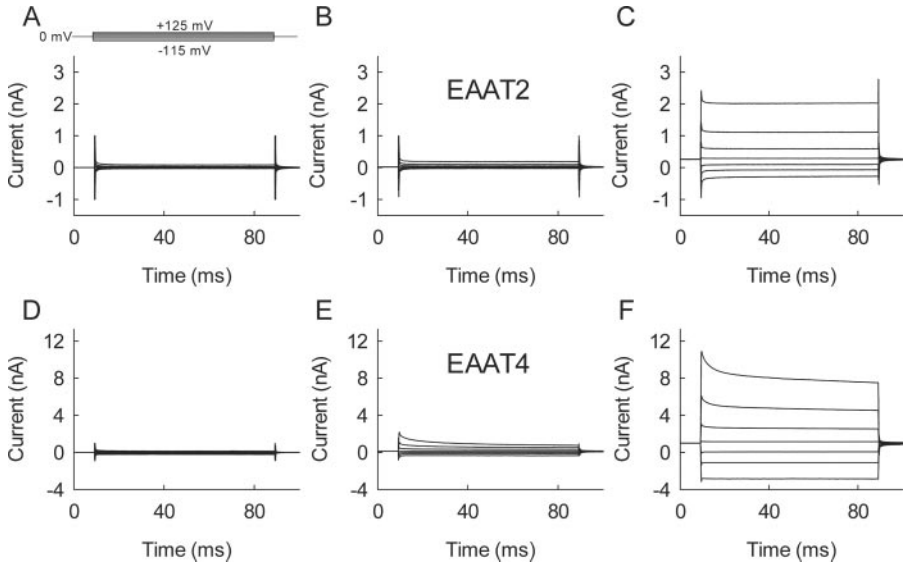

FIG. 1. **Constitutive anion currents in cells expressing EAAT2 or EAAT4.** Representative whole-cell current traces recorded from tsA201 cells expressing EAAT2 (*A–C*) and EAAT4 (*D–F*) transporters. Cells were dialyzed with a NaCl-based internal solution and perfused with a glutamate-free external solution containing Cl^- (*A* and *D*), NO_3^- (*B* and *E*), or SCN^- (*C* and *F*) as main anions. Cells were held at 0 mV, and voltage steps between −115 and +125 mV in 40-mV intervals were applied.

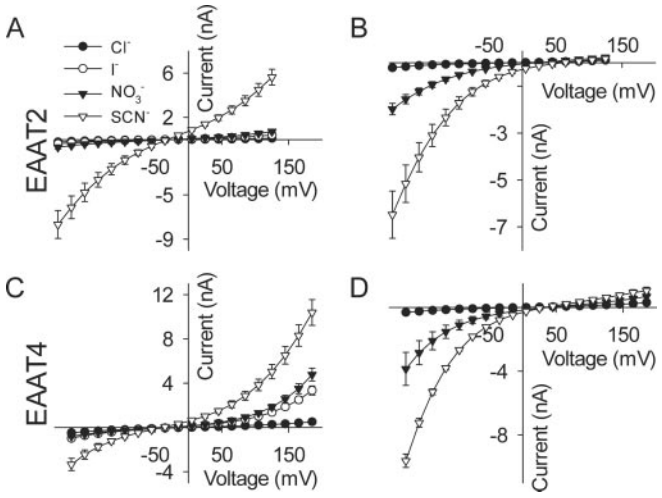

FIG. 2. **Anion selectivity of EAAT2- and EAAT4-associated anion channels.** *A* and *C*, voltage dependence of isochronal current amplitudes determined for different external anion compositions. Current amplitudes were measured in an external solution containing Cl^-, I^-, NO_3^-, or SCN^- as the principal anions, in cells expressing EAAT2 (*A*) and EAAT4 (*C*). Cells were dialyzed with a standard NaCl-based internal solution. *B* and *D*, voltage dependence of isochronal current amplitudes for different internal anion compositions. Current amplitudes were measured in cells dialyzed with a solution containing Cl^-, NO_3^-, or SCN^- as the principal anions, in cells expressing EAAT2 (*B*) and EAAT4 (*D*). The external solution had the standard composition. Means ± S.E. of absolute current data from at least 5 cells for all figures.

TABLE I
Relative permeabilities and conductivities for external anions

			internal Na^+					
			E_{rev}(mV)	P_X/P_{Cl}	N	I_X/I_{NO3} at +125mV	I_X/I_{NO3} at - 175mV	N
0.0 mM glutamate	EAAT2	Cl	-	-	-	0.3 ± 0.0	0.8 ± 0.1	8
		I	-41 ± 2.2	4.2 ± 0.4*	6	0.9 ± 0.08	1.2 ± 0.08	4
		NO_3	-27 ± 4.9	2.5 ± 0.5▲	4	-	-	-
		SCN	-33 ± 2.9	3.3 ± 0.4▲▲	8	8.8 ± 1.1	15.9 ± 4.0	7
	EAAT4	Cl	-	-	-	0.1 ± 0.0	0.4 ± 0.1	14
		I	-29.9 ± 2.2	2.7 ± 0.2▲▲	8	0.6 ± 0.1▲	1.0 ± 0.2▲	12
		NO_3	-30.3 ± 1.9	2.9 ± 0.2▲▲**	14	-	-	-
		SCN	-45.7 ± 1.5	5.0 ± 0.3▲**	11	3.2 ± 0.4	3.9 ± 0.4	8
0.5 mM glutamate	EAAT2	Cl	-	-	-	0.2 ± 0.0	0.6 ± 0.1	8
		I	-44.3 ± 2.4	4.8 ± 0.5**	6	0.64 ± 0.06	0.69 ± 0.07	4
		NO_3	-35 ± 3.3	3.4 ± 0.5▲**	4	-	-	-
		SCN	-28.1 ± 3.6	2.8 ± 0.4▲▲	8	6.6 ± 0.8	9.3 ± 1.1	7
	EAAT4	Cl	-	-	-	0.1 ± 0.0	0.4 ± 0.0	14
		I	-43.1 ± 1.6	3.7 ± 0.3▲▲**	8	0.4 ± 0.0▲*	0.6 ± 0.1▲*	12
		NO_3	-43.7 ± 1.3	4.7 ± 0.2▲▲**	14	-	-	-
		SCN	-41.8 ± 1.9	4.4 ± 0.3▲**	11	3.0 ± 0.2	4.8 ± 0.6	8
			internal K^+					
0.0 mM glutamate	EAAT2	Cl	-	-	-	0.4 ± 0.0▲▲	0.8 ± 0.0	16
		I	-27 ± 2.7	2.3 ± 0.3▲*	7	0.7 ± 0.0	1.0 ± 0.2	3
		NO_3	-31 ± 2.5	3.3 ± 0.3▲▲	14	-	-	-
		SCN	-39 ± 2.5	4.0 ± 0.5▲▲	9	6.7 ± 0.6	8.5 ± 1.7	7
	EAAT4	Cl	-	-	-	0.2 ± 0.0	0.3 ± 0.1	12
		I	-29.9 ± 2.2	2.7 ± 0.2▲▲	7	0.9 ± 0.3	1.1 ± 0.3	7
		NO_3	-19.5 ± 1.5	1.8 ± 0.1▲▲**	11	-	-	-
		SCN	-28.6 ± 2.3	2.6 ± 0.2▲▲**	10	4.0 ± 0.3	5.4 ± 1.1	5

(Table II). Similar experiments with EAAT4 (Fig. 2, *C* and *D*) demonstrated an $SCN > NO_3 > I > Cl$ conductivity and permeability sequence for external as well as for internal anions (Tables I and II).

EAAT2- and EAAT4-associated anion currents differ in the relative anion conductivities as well as in the relative anion permeabilities (Tables I and II), in the absolute current amplitude (Fig. 2) and in the time and voltage dependence of the current amplitude. These differences dismiss the possibility that anion currents measured in the absence of glutamate are conducted by endogenous anion channels up-regulated by overexpression of EAAT transporters and provide evidence that anion pores are formed by EAAT proteins either in homomeric or in heteromeric complexes together with endogenous proteins.

Transitions in the Glutamate Transport Cycle Modify EAAT-associated Anion Pathways—Application of external glutamate enhanced EAAT-associated anion currents and modified the underlying anion channels. Fig. 3 shows EAAT4-associated current amplitudes in the absence and in the presence of glutamate under two ionic compositions: NaCl-based internal and $NaNO_3$-based external solutions (Fig. 3, *A* and *C*) and $NaNO_3$-based internal and NaCl-based external solutions (Fig. 3, *B* and *D*). For both conditions, application of external glutamate caused about a 2-fold increase of the anion current amplitude (Fig. 3, *C* and *D,* and Fig. 4*A*). Similar increases of the anion current amplitude by glutamate are observed in cells expressing EAAT2 (Fig. 4*A*). This demonstrates that there is a substantial constitutive activity of EAAT anion channels in the absence of glutamate.

TABLE II
Relative anion permeabilities for internal anions

▲, statistical significance of differences in permeability ratios between perfusion with and without glutamate based on a Student's *t* test. *, statistical significance of differences in permeability ratios between cells dialyzed with K^+ and Na^+ based on a Student's *t* test (number of symbols denotes the level of significance: one symbol indicates $p < 0.05$; two symbols indicates $p < 0.01$).

			internal Na^+		
			E_{rev} (mV)	P_X/P_{Cl}	N
0.0 mM Glu	EAAT2	NO_3	26.5 ± 7.5	3.7 ± 0.9▲	5
		SCN	72.5 ± 7.2	26.2 ± 6.0▲**	6
	EAAT4	NO_3	33.6 ± 2.1	5.0 ± 0.5▲	5
		SCN	37.9 ± 5.1	6.5 ± 1.5▲▲	7
0.5 mM Glu	EAAT2	NO_3	41.0 ± 8.4	6.8 ± 1.6▲	5
		SCN	95.5 ± 8.3	67.2 ± 16.5▲**	6
	EAAT4	NO_3	49.6 ± 3.3	9.3 ± 1.14▲	5
		SCN	61.3 ± 4.9	15.9 ± 3.0▲▲	7
			internal K^+		
0.0 mM Glu	EAAT2	NO_3	10.0 ± 2.5	2.0 ± 0.2▲▲	7
		SCN	47.0 ± 2.2	6.0 ± 0.8▲▲**	4
	EAAT4	NO_3	26.7 ± 3.7	3.9 ± 0.5▲▲	7
		SCN	47.4 ± 4.5	9.8 ± 2.3▲▲	10

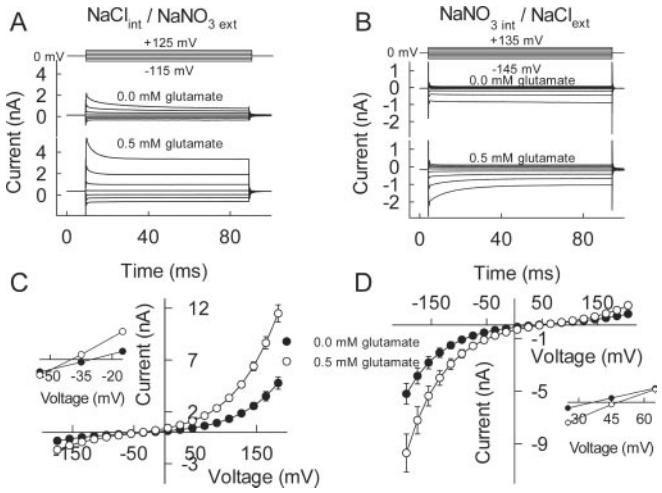

FIG. 3. **Application of external glutamate increases macroscopic current amplitudes and modifies functional properties of EAAT anion channels.** *A* and *B*, representative whole-cell current traces recorded from tsA201 cells expressing EAAT4 transporters intracellularly dialyzed with NaCl-based solution but perfused with a $NaNO_3^-$-based solution (*A*), or from cells intracellularly dialyzed with a $NaNO_3^-$-based solution in NaCl-based external solution (*B*) before and after external application of 0.5 mM glutamate. *C* and *D*, corresponding mean current amplitudes before (●) and after (○) external application of 0.5 mM glutamate from cells intracellularly dialyzed with NaCl-based solution, but perfused with a $NaNO_3^-$-based solution (*C*) and from cells intracellularly dialyzed with a $NaNO_3^-$-based solution in standard external solution (*D*). *Insets*, glutamate causes a shift of the anion current reversal potential. Mean ± S.E. from 5 cells.

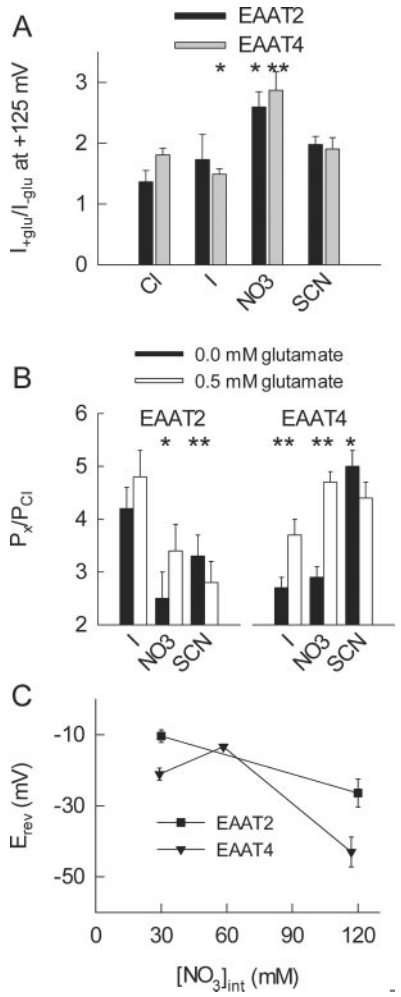

FIG. 4. **Glutamate alters anion conduction properties of EAAT transporters.** *A*, current ratios of isochronal current amplitudes before and after external application of 0.5 mM glutamate at +125 mV obtained from cells expressing EAAT2 (n = 3–14) or EAAT4 (n = 4–7). Cells were dialyzed with a standard NaCl-based internal solution and perfused with solutions containing either Cl^-, I^-, NO_3^-, or SCN^- as principal anions. * and ** indicate statistically significant differences based on a Student's *t* test (*, $p < 0.05$; **, $p < 0.01$). *B*, glutamate-induced changes of the anion permeability ratio for EAAT-2 and EAAT-4 in the absence of internal potassium. *C*, the EAAT-associated anion conductance is mediated by a multiply occupied pore. Dependence of the current reversal potential on the absolute anion concentration in cells expressing EAAT2 (■, n = 9) or EAAT4 (▼, n = 3). The concentration of $[NO_3^-]_i$ and $[SCN]_e$ was altered in a way that the concentration ratio stayed constant. The measured reversal potentials were different at $p < 0.01$.

EAAT4-associated anion currents display distinct time and voltage dependences for various anionic conditions. For NaCl-based internal and $NaNO_3$-based external solutions, there was a time-dependent current decrease at positive potentials (Fig. 3*A*). In contrast, for $NaNO_3$-based internal and NaCl-based external solution, currents activated upon membrane hyperpolarization (Fig. 3*B*). Glutamate caused a change of the time and voltage dependence of currents for both anion conditions. Current inactivation was less pronounced in the presence of glutamate in external NO_3^- (Fig. 3*A*), and for internal NO_3^- a time-dependent current decrease at negative potentials appeared after glutamate application (Fig. 3*B*). EAAT2 anion currents did not exhibit time-dependent changes of the current amplitude for external (Fig. 1) or for internal NO_3^- (data not shown).

For EAAT2 and EAAT4, the glutamate-induced current increase depended on the anion composition. For cells intracellularly dialyzed with a NaCl-based internal solution, these values were highest for NO_3^- and smaller for SCN^-, I^-, and Cl^- (Fig. 4*A*). Moreover, for various ionic conditions application of glutamate caused a significant shift of the reversal potential (Fig. 3, *C* and *D, insets*, Tables I and II). These shifts were not due to glutamate permeation through the anion pore, as glutamate caused shifts to more negative under certain conditions (Fig. 3*C, inset*) and shifts to more positive potentials under others (Fig. 3*D, inset*). They rather indicate an alteration of the relative anion permeability of EAAT2- and EAAT4-associated anion pathways by glutamate (Fig. 4*B*).

Other steps in the glutamate transport cycle (20, 26–28) also altered the selectivity of the anion pores. Internal solutions without K^+ prevent the occupation of K^+-bound states and might therefore result in a distinct distribution of transporter states than under standard conditions (20). If all anion conducting states displayed the same anion permeability, the reversal potentials determined with the two distinct internal solutions would be identical. In contrast, differences in measured reversal potentials indicate that distinct conformations of EAAT transporters are associated with different anion permeabilities. For EAAT2 and EAAT4, the anion permeability ratios for certain external anions measured in the absence of glutamate depended on the intracellular cation. The relative permeability of EAAT2 for external I^- and for internal SCN^- was significantly different for cells dialyzed with Na^+ or K^+ (Table I). For EAAT4, distinct anion permeabilities for external SCN^- and NO_3^- but for none of the tested internal anions were observed (Table I). These results indicate that various conformational states of EAAT2 and EAAT4 are associated with distinct anion selectivities.

EAAT2 and EAAT4 Exhibit Multiply Occupied Anion-selective Pores—The EAAT-associated anion conductance exhibited several properties that appear unusual for a pore-mediated process: an increase of Cl^- efflux upon application of more permeant external anions (Fig. 2) comparable with a trans-acceleration phenomenon, a change of permeability and conductivity upon addition of glutamate (Figs. 3 and 4, Tables I and II), and the dependence of anion selectivity on the intracellular cation (Tables I and II). These observations could cast some doubt on the notion that the EAAT-anion conductance is pore-mediated. The concentration dependence of the reversal potential under biionic conditions is a very sensitive test for ion conduction by a multiply occupied ion pore (29). By using two permeant anions, SCN^- and NO_3^-, we recorded reversal potentials under biionic conditions with a fixed concentration ratio for various absolute concentrations. As $Glu/Na^+/H^+/K^+$ currents are absent and anion current amplitudes are significantly larger than endogenous currents, reversal potentials reflect the relative anion permeability of the EAAT-associated anion conductance. In both isoforms, reversal potentials shifted upon reduction of the absolute anion concentration, although the ratio of the anion concentrations at both sides of the membrane stayed constant (Fig. 4*C*). This demonstrated that anion transport does not occur in a fixed stoichiometry and excluded a carrier-mediated anion transport. Moreover, it indicated that the anion pores of EAAT2 and EAAT4 contain more than one anion.

External Glutamate Modifies the Transfer of Anions through EAAT-associated Pores—The observed changes of anion conduction (Fig. 4) suggest that certain steps in anion permeation through the EAAT anion pores are altered by external substrate. To test which of these steps are primarily affected by external glutamate, we determined the effects of varying the external $[SCN^-]$ composition on the EAAT-associated anion current. Experiments were performed in the absence (Fig. 5*A*) and in the presence of external glutamate (Fig. 5*B*). For both conditions, the current amplitude-$[SCN^-]$ plot could be well fit with a Michaelis-Menten relationship with a Hill coefficient of 1 revealing SCN^- dissociation constants (K_D) for various voltages (Fig. 5, *C* and *D*). External substrate increased the K_D values about 2-fold at positive potentials (Fig. 5*C*) but left them unaltered at negative voltages (Fig. 5*D*).

Our analysis was performed at voltages more than 80 mV away from the current reversal potential. Under these conditions, anion influx through a multiply occupied pore greatly exceeds anion efflux at positive potentials and is negligible at

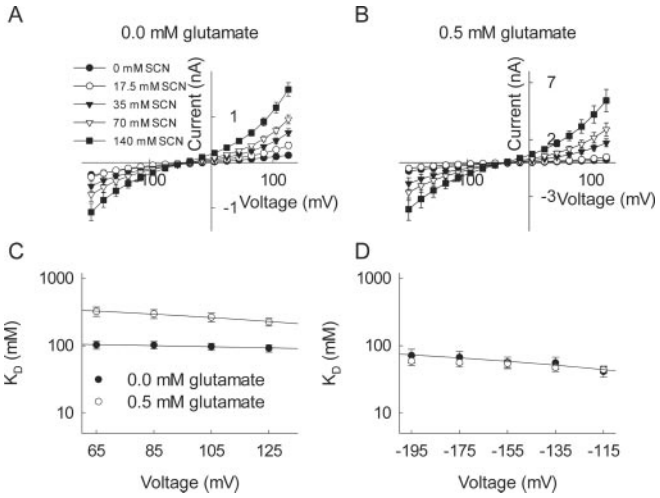

FIG. 5. **Effect of changes of $[SCN^-]_o$ on isochronal current amplitudes in tsA201 cells expressing EAAT2.** *A*, mean current amplitudes for various external $[SCN^-]$ in the absence of external glutamate. SCN^- was substituted equimolarly with Cl^-. *B*, mean current amplitudes for various external $[SCN^-]$ in the presence of 0.5 mM external glutamate. *C* and *D*, voltage dependence of the K_D for SCN^- in the absence (●) and in the presence (○) of external glutamate. Means ± S.E. from 7 cells.

negative potentials ($(j_{eff}/j_{in}) = e^{-n(VF/RT)}$, where n is the number of simultaneously binding ions and V the transmembrane voltage (30)). The concentration dependence of the current amplitude thus gives the concentration dependence of the SCN^- influx at positive potentials or of the Cl^- efflux at negative potentials. Saturation of the ion flux with increasing external $[SCN^-]$ can occur when the binding-unbinding step to a first binding site within the ion conduction pathway becomes rate-limiting. This happens when the rate of entry approaches the maximum rate of the unbinding step. As unbinding can be followed either by diffusing into the external solution or by translocation through the pore, binding of external SCN^- can be described by three distinct rate constants: the binding constant (k_{on}), the rate constant of unbinding and passing through the pore (k_{trans}), and the rate constant of unbinding and diffusing into the external solution (k_{off}) ($K_D = (k_{off} + k_{trans})/k_{on}$). The observed glutamate and voltage dependence of the SCN^- dissociation constants can be nicely explained by assuming that external glutamate accelerates the translocation step for external SCN^-. This assumption correctly predicts that glutamate increases the SCN^- influx (Fig. 4*A*) as well as the measured K_D values at positive potentials (Fig. 5*C*). It is also in agreement with the unchanged dissociation constants at negative potentials (Fig. 5*D*). Most likely, at negative potentials the k_{trans} rate constant (describing a transition against the electrostatic gradient) is substantially smaller than at positive potentials. Its contribution to the dissociation constants at negative membrane potentials will therefore be negligible. Thus, a glutamate-induced change of k_{trans} will only little affect the K_D values at negative potentials, in agreement with the experimental results (Fig. 5*D*). The glutamate-induced acceleration of the k_{trans} rate constant predicts an increase of the unitary current amplitude, providing a novel explanation for the increase of the macroscopic current amplitude in the presence of substrate.

Unitary Properties of EAAT4-associated Anion Channels—In external I^-, NO_3^-, and SCN^-, EAAT4-associated anion currents displayed prominent time- and voltage-dependent current relaxations in both the absence and the presence of external glutamate (Figs. 1 and 3). These transient currents are not capacitive charge movements; they are changes of ionic current

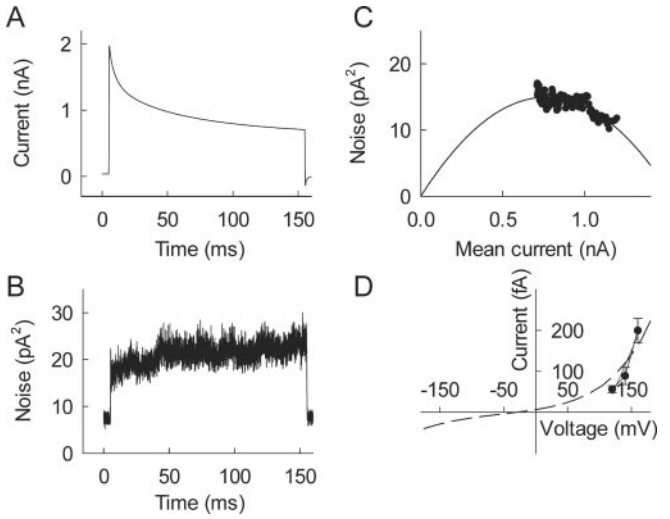

FIG. 6. **Variance analysis for EAAT4 anion channels.** *A*, mean current trace obtained from 300 current responses to a test step to +120 mV from a holding potential of −53 mV. *B*, time course of the variance. *C*, variance *versus* current plot fitted to the function $\sigma^2 = iI(t) - I(t)^2/N$ (*solid line*). *D*, voltage dependence of the unitary current amplitudes for three different test potentials (●). The *dashed line* represents the current-voltage relationship of the instantaneous macroscopic current from 6 cells measured under identical conditions scaled down to superimpose on the single channel currents. All data were obtained from cells dialyzed with a standard intracellular solution and extracellularly perfused with $NaNO_3$-based solution.

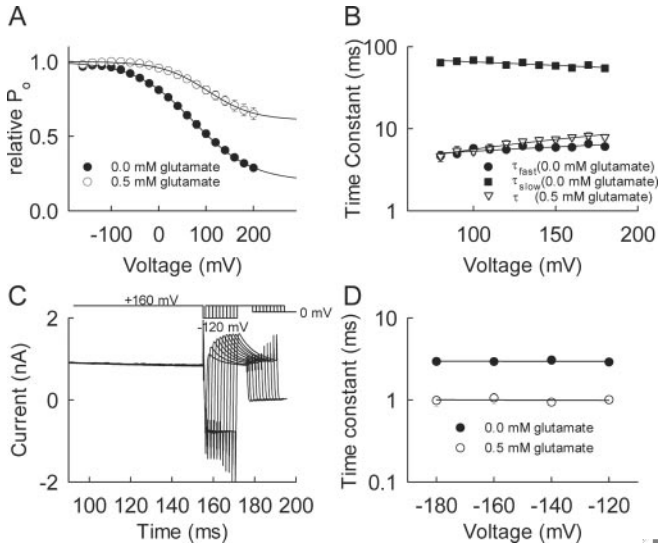

FIG. 7. **Time- and voltage-dependent changes of EAAT4-associated anion currents.** *A*, voltage dependence of the relative open probability of the EAAT4 anion channels in the absence (●, $n = 7$) and in the presence of 0.5 mM glutamate (○, $n = 7$). *B*, voltage dependence of time constants of inactivation in the absence (●, ■ $n = 31$) and in the presence (○, $n = 31$) of 0.5 mM glutamate. *C*, current response of a tsA201 cell expressing EAAT4 to a pulse protocol consisting of a pulse to +160 mV followed by a voltage step −120 mV of variable duration and a fixed test step to +160 mV. *D*, voltage dependence of the time constants of the recovery from inactivation in the absence (●, $n = 7$) and in the presence of 0.5 mM glutamate (○, $n = 5$). All data were obtained from cells dialyzed with a standard intracellular solution and extracellularly perfused with $NaNO_3$-based solution.

amplitudes as illustrated by the following three pieces of evidence: the amplitude differed for distinct anions (Figs. 1 and 2), the reversal potential shifted upon alterations of the anion composition (Fig. 3), and integrals of the transient currents elicited by steps to positive potentials were always distinct from the integral determined after stepping back to the holding potential. The observed current relaxations therefore can be caused by two distinct mechanisms: time-dependent changes of the open probability of the anion channel or decreases of the unitary current amplitude. We employed non-stationary noise analysis to distinguish between the two possibilities.

Fig. 6 shows variance analysis from a tsA201 cell expressing EAAT4 dialyzed with NaCl-based internal solution in a $NaNO_3$-based external solution. Fig. 6, *A* and *B,* illustrates the time course of the average current for a voltage step from the current reversal potential (−53 mV) to a test potential of +120 mV and the corresponding time course of the variance. Although the current amplitude decreased with time after the voltage step, the noise increased. Such a time dependence of the current amplitude and the noise ($\sigma^2 = Ni^2\,P(1 - P) = (I^2/N)(1/P - 1)$) indicates that the EAAT4-associated current relaxations are due to changes of the number of open channels. Gating of EAAT4 occurs by the same mechanism as gating of ion channels.

To obtain the unitary current amplitude and the absolute open probability of the underlying channels, the variance-mean current plot in Fig. 6*C* was fitted to Equation 3. From this fit, the unitary current amplitude, 57 ± 7 fA ($n = 9$) at +120 mV, and the number of channels in the cell were obtained. By dividing the instantaneous current amplitude by the product of the unitary current amplitude and the number of channels, we then calculated the absolute open probability at the holding potential (0.84 ± 0.06, $n = 9$)). Measurements were repeated in several cells at three different test potentials (Fig. 6*D*).

Because the open probability of EAAT4 is distinct from zero at the end of the test pulse, the variance-mean current plot is not a complete parabola. However, as the fitted parabola assumed its maximum within the experimentally determined variance-mean current plot, the fits were well defined. We obtained reproducible results for the unitary current amplitude and the open probabilities at the beginning and the end of the voltage step in several cells. All these results demonstrated that our non-stationary noise analysis reliably determined the unitary current amplitude of EAAT4. The high absolute open probability of EAAT4 anion channels in glutamate-free solutions demonstrates that a mere increase of the open probability cannot explain the glutamate-induced increase of the macroscopic current amplitude. Obviously, glutamate also increases the unitary current amplitude of EAAT4 anion channels.

Gating of EAAT4-associated Anion Channels—We next studied time- and voltage-dependent opening and closing transitions of EAAT4-associated anion channels in cells dialyzed with NaCl-based internal solution in a $NaNO_3$-based external solution. In the absence of glutamate, steady-state inactivation can be described with a single Boltzmann distribution with a midpoint of inactivation at 75.4 ± 9.2 mV ($n = 7$) and a voltage-dependent minimum open probability of 0.19 ± 0.02 ($n = 7$) (Fig. 7*A*). The significant minimum open probability can be assigned to an incomplete inactivation of EAAT4 anion channels by noise analysis (Fig. 6*C*). Current amplitudes decayed in a biexponential time course with two time constants of about 5 and 60 ms (Fig. 7*B*). Stepping back to negative potentials after a positive test step caused a monoexponential increase of the amplitude of the currents elicited by a following step to +160 mV (Fig. 7, *C* and *D*).

Voltage-dependent gating of EAAT4 anion channels is modified by external glutamate. Addition of external glutamate increased the minimum open probability to 0.60 ± 0.05 ($n = 7$) and shifted the midpoint of inactivation to 106.3 ± 3.2 mV ($n = 7$) (Fig. 7*A*). Before application of glutamate, currents decayed in a biexponential time course at positive potentials (Fig. 7*B*). After application of 0.5 mM glutamate, the current decay became monoexponential with a time constant of about 5 ms and

a significantly increased relative late current amplitude, *i.e.* a significant increase of the ratio of the late by the instantaneous current amplitude at positive potentials (Fig. 7, *A* and *B*). Furthermore, glutamate decreased the time constants of recovery from inactivation (Fig. 7*D*). The glutamate-induced gating alterations will result in an increase of the EAAT4 anion conductance under various conditions. In the absence as well as in the presence of external glutamate, membrane depolarization might cause an inactivation of EAAT-associated anion channels. In the presence of glutamate, this inactivation will be less complete and recovered faster after returning to the resting potential causing a decreased input resistance and membrane length constant.

DISCUSSION

EAAT-associated Anion Currents—The small background anion permeability of our expression system enabled us to measure directly EAAT-associated anion currents in the absence as well as in the presence of external substrate. For both isoforms, anion currents were significantly different from currents observed in untransfected cells. Application of external glutamate caused a 2-fold increase of the anion current amplitude (Fig. 4*A*) indicating that EAAT-associated anion channels are active in the absence of substrate and that this tonically active anion conductance is a substantial component of the activated anion current (Figs. 3 and 4). The existence of a glutamate-independent anion conductance has been reported (15, 31, 32); however, previous estimates of the relative amplitude of this current amplitude for EAAT1 and EAAT3 were much lower (between 0.05 and 0.2 (15, 32)). This difference likely arises from the methods used to measure the glutamate-independent anion currents. Earlier experiments employed blocking agents to estimate the glutamate-independent anion conductance. It appears possible that block of the anion conductance by these agents is incomplete resulting in an underestimation of the substrate-independent conductance. In contrast, we determined current amplitudes without subtraction procedures. As anion currents are potentially contaminated by currents conducted by endogenous anion channels, our estimate of the tonically active EAAT-associated anion currents might be above the real value. For measurements with Cl^- as the only permeant anion, currents associated with EAAT2 are quite small, and indeed the glutamate-induced current increase determined under these conditions is smaller than the values for other anions (Fig. 4*A*). However, for other experimental conditions, the contribution of endogenous anions currents appears to be negligible for the following experimental results. The substrate-independent anion currents in EAAT2 and EAAT4-expressing cells differ in selectivity (Table I) and display a distinct time and voltage dependence of the current amplitude (Fig. 1), demonstrating that the anion currents are conducted by distinct heterologously expressed anion channels. Moreover, if a significant component of the substrate-independent anion current were conducted by endogenous channels, one would expect that the relative glutamate-induced anion current increases differ for varying expression levels of the EAAT protein, which was not observed in our experiments with I^-, NO_3^-, or SCN^- as permeant anions.

Anion Selectivity of EAAT-associated Pores—For EAAT2 and EAAT4, larger and polyatomic anions display a higher permeability and conductivity than Cl^-. The mechanisms underlying this particular anion selectivity of EAAT-associated anion channels are currently not very well understood. However, a comparison with a different class of anion-selective channels, the ClC family of voltage-gated chloride channels, allows us insights into the processes that are involved in anion permeation and selection between different anions. ClC channels, similar to every anion channel tested so far, exhibit pores with anion-binding sites that prefer large and polyatomic anions (34). There are two classes of ClC channels that differ in the selectivity between anions, isoforms with a $Cl^- > NO_3^-$ and isoforms or mutant channels exhibiting an $NO_3^- > Cl^-$ permeability and conductivity sequence. These two classes of ClC channels do not differ in the selectivity of binding but in the absolute binding interaction energy for anions (34). For example, in ClC-1, a ClC isoform with a $Cl^- > NO_3^-$ anion permeability and conductivity sequence, binding of anions is tight. Therefore, larger and polyatomic anions dwell longer than small anions at the anion-binding sites. This reduces the permeability of these anions and causes the block of chloride current (35, 36). In contrast, in ClC-4, exhibiting a $NO_3^- > Cl^-$ permeability sequence, the interaction energy is substantially lower. Association steps to the binding sites are rate-limiting and thus permeability follows the binding selectivity of the anion-binding sites (18). For EAAT2 and EAAT4, we found no indication of block by permeating anions. Apparently, for both anion pores, anion binding is less tight than in ClC channels resulting in the observed $SCN^- > NO_3^- > I^- > Cl^-$ conductivity sequence.

EAAT4-associated Anion Channels Have a Small Unitary Conductance and a High Open Probability in Substrate-free Solution—By using non-stationary noise analysis, we determined unitary current amplitudes of EAAT4 anion channels in the fA range (Fig. 6*D*). By taking the distinct voltages and anion composition into account, these results are significantly larger than published unitary current amplitudes for EAAT1 (15) and smaller than those reported for a native glutamate transporter in photoreceptors from the tiger salamander (12) and heterologously expressed EAAT5 (33). We do not know the reasons for these differences. They might be caused by isoform-specific differences in anion conductance, but they could also be due to the distinct experimental procedures employed. The earlier results were obtained by applying various concentrations of glutamate assuming that the open probability in the absence of substrate is close to zero. If the studied glutamate transporter-associated anion channels exhibited comparably large open probabilities in the absence of substrate as EAAT4, it could be that EAAT current amplitudes and variances have been subtracted by these procedures.

A Substrate-modified Anion Pore in EAAT2 and EAAT4—For EAAT2 and EAAT4, glutamate application alters the current reversal potentials under various asymmetric anion conditions (Figs. 3 and 4 and Tables I and II) indicating changes of the selectivity of the EAAT-associated anion channels. Experiments on cells dialyzed with either K^+-containing or K^+-free solution demonstrated that not only binding of glutamate but also other steps in the glutamate uptake cycle modify the anion selectivity of the EAAT anion pore. The finding that conformational changes of the glutamate carrier domain cause alterations of the anion selectivity filter suggests a close spatial proximity of glutamate transport and anion pore.

Comparing dissociation constants for SCN^- in the absence and in the presence of glutamate revealed that the K_D values at positive voltages were increased by application of substrate but unaffected in the negative range (Fig. 4), in agreement with the notion that glutamate increases the rate constant for transversing the pore. These results suggest that glutamate causes an augmentation of the unitary current amplitude. This idea is supported by the high absolute open probability of EAAT4 anion channels in the absence of glutamate (0.84 ± 0.06, $n = 9$ at -53 mV). An increase of the open probability alone cannot explain the 3-fold increase of the macroscopic current amplitude by glutamate under these conditions (Figs. 3*A* and 4*A*).

A Glutamate-modified Voltage-gated Anion Channel—So far, EAAT-associated anion channels have been thought to be gated by a tight coupling to the glutamate carrier domain. Opening and closing were assumed to be governed by transitions in the glutamate uptake cycle resulting in gating features that are very similar to ligand-gated channels. Our results demonstrate certain discrepancies to this concept. EAAT-associated anion channels exhibit a substantial open probability in the absence of glutamate transport. Moreover, voltage-dependent gating of EAAT4 illustrates opening and closing transitions that are independent of transitions in the glutamate uptake cycle. These gating transitions are modified by glutamate in a way favoring the conducting state, *i.e.* by increasing the voltage-independent open probability (Fig. 5) and accelerating the recovery from inactivation (Fig. 5). In the presence as well as in the absence of substrate, gating of EAAT4 depends on the anion composition (Fig. 3, *A* and *B*), quite similar to other anion channels, such as ClC-type (37, 38) or volume-activated anion channels (39).

Our results suggest a new view of EAAT-associated anion channels. They function as voltage-dependent anion channels much like conventional anion channels, but the functional properties are altered by the glutamate carrier domain. This modification not only alters transitions between conducting and non-conducting states but also affects pore properties, in clear contrast to almost all known examples of a modification of an ion channel by a ligand-bound receptor.

Acknowledgements—We thank Dr. M. Hediger and Dr. J. Rothstein for providing expression constructs for hEAAT2 and rEAAT4; Dr. Patricia Hidalgo and Dr. J. P. Johnson for critical review of the manuscript and helpful discussions; Dr. Louis DeFelice for helpful discussions; and Hannelore Heidtmann and Barbara Poser for excellent technical assistance.

REFERENCES

1. Takahashi, M., Billups, B., Rossi, D., Sarantis, M., Hamann, M., and Attwell, D. (1997) *J. Exp. Biol.* **200,** 401–409
2. Seal, R. P., and Amara, S. G. (1999) *Annu. Rev. Pharmacol. Toxicol.* **39,** 431–456
3. Kanner, B. I. (1994) *J. Exp. Biol.* **196,** 237–249
4. Kanai, Y., and Hediger, M. A. (1992) *Nature* **360,** 467–471
5. Pines, G., Danbolt, N. C., Bjoras, M., Zhang, Y., Bendahan, A., Eide, L., Koepsell, H., Storm-Mathisen, J., Seeberg, E., and Kanner, B. I. (1992) *Nature* **360,** 464–467
6. Storck, T., Schulte, S., Hofmann, K., and Stoffel, W. (1992) *Proc. Natl. Acad. Sci. U. S. A.* **89,** 10955–10959
7. Arriza, J. L., Fairman, W. A., Wadiche, J. I., Murdoch, G. H., Kavanaugh, M. P., and Amara, S. G. (1994) *J. Neurosci.* **14,** 5559–5569
8. Arriza, J. L., Eliasof, S., Kavanaugh, M. P., and Amara, S. G. (1997) *Proc. Natl. Acad. Sci. U. S. A.* **94,** 4155–4160
9. Fairman, W. A., Vandenberg, R. J., Arriza, J. L., Kavanaugh, M. P., and Amara, S. G. (1995) *Nature* **375,** 599–603
10. Zerangue, N., and Kavanaugh, M. P. (1996) *Nature* **383,** 634–637
11. Levy, L. M., Warr, O., and Attwell, D. (1998) *J. Neurosci.* **18,** 9620–9628
12. Larsson, H. P., Picaud, S. A., Werblin, F. S., and Lecar, H. (1996) *Biophys. J.* **70,** 733–742
13. Wadiche, J. I., Amara, S. G., and Kavanaugh, M. P. (1995) *Neuron* **15,** 721–728
14. Billups, B., Rossi, D., and Attwell, D. (1996) *J. Neurosci.* **16,** 6722–6731
15. Wadiche, J. I., and Kavanaugh, M. P. (1998) *J. Neurosci.* **18,** 7650–7661
16. Trotti, D., Rolfs, A., Danbolt, N. C., Brown, R. H., Jr., and Hediger, M. A. (1999) *Nat. Neurosci.* **2,** 427–433
17. Lin, C. L., Tzingounis, A. V., Jin, L., Furuta, A., Kavanaugh, M. P., and Rothstein, J. D. (1998) *Brain Res.* **63,** 174–179
18. Hebeisen, S., Heidtmann, L., Cosmelli, D., Gonzalez, C., Latorre, R., Alvarez, O., and Fahlke, Ch. (2003) *Biophys. J.* **84,** 2306–2318
19. Jurman, M. E., Boland, L. M., Liu, Y., and Yellen, G. (1994) *BioTechniques* **17,** 876–881
20. Bergles, D. E., Tzingounis, A. V., and Jahr, C. E. (2002) *J. Neurosci.* **22,** 10153–10162
21. Barry, P. H. (1994) *J. Neurosci. Methods* **51,** 107–116
22. Neher, E. (1992) *Methods Enzymol.* **207,** 123–131.
23. DeFelice, L. J. (1981) in *Introduction to Membrane Noise* (DeFelice, L. J., ed) pp. 291–323, Plenum Publishing Corp., New York
24. Sigworth, F. J. (1980) *J. Physiol. (Lond.)* **307,** 97–129
25. Heinemann, S. H., and Conti, F. (1992) *Methods Enzymol.* **207,** 131–148
26. Otis, T. S., and Jahr, C. E. (1998) *J. Neurosci.* **18,** 7099–7110
27. Watzke, N., Bamberg, E., and Grewer, C. (2001) *J. Gen. Physiol.* **117,** 547–562
28. Auger, C., and Attwell, D. (2000) *Neuron* **28,** 547–558
29. Dani, J. A. (1989) *J. Neurosci.* **9,** 884–892
30. Hodgkin, A. L., and Keynes, R. D. (1955) *J. Physiol. (Lond.)* **128,** 61–88
31. Eliasof, S., and Jahr, C. E. (1996) *Proc. Natl. Acad. Sci. U. S. A.* **93,** 4153–4158
32. Watzke, N., and Grewer, C. (2001) *FEBS Lett.* **503,** 121–125
33. Palmer, M. J., Taschenberger, H., Hull, C., Tremere, L., and von Gersdorff, H. (2003) *J. Neurosci.* **23,** 4831–4841
34. Fahlke, Ch. (2001) *Am. J. Physiol.* **280,** F748–F757
35. Fahlke, Ch., Dürr, C., and George, A. L., Jr. (1997) *J. Gen. Physiol.* **110,** 551–564
36. Rychkov, G. Y., Pusch, M., Roberts, M. L., Jentsch, T. J., and Bretag, A. H. (1998) *J. Gen. Physiol.* **111,** 653–665
37. Richard, E. A., and Miller, C. (1990) *Science* **247,** 1208–1210
38. Pusch, M., Ludewig, U., Rehfeldt, A., and Jentsch, T. J. (1995) *Nature* **373,** 527–530
39. Voets, T., Droogmans, G., and Nilius, B. (1997) *J. Gen. Physiol.* **110,** 313–325

Nico Melzer, Delany Torres-Salazar, Christoph Fahlke

A dynamic switch between inhibitory and excitatory currents in a neuronal glutamate transporter

Proceedings of the National Academy of Sciences USA 2005

A dynamic switch between inhibitory and excitatory currents in a neuronal glutamate transporter

Nico Melzer*†, Delany Torres-Salazar*†, and Christoph Fahlke*†‡§

*Abteilung Neurophysiologie, Medizinische Hochschule Hannover, Carl-Neuberg-Strasse 1, 30625 Hannover, Germany; †Abteilung Physiologie, Rheinisch-Westfälische Technische Hochschule Aachen, Pauwelsstrasse 30, 52074 Aachen, Germany; and ‡Centro de Estudios Cientificos (CECS), Arturo Prat 514, Valdivia, Chile

Edited by Susan G. Amara, University of Pittsburgh School of Medicine, Pittsburgh, PA, and approved November 8, 2005 (received for review October 9, 2005)

Excitatory amino acid transporters (EAATs) terminate glutamatergic synaptic transmission and maintain extracellular glutamate concentrations in the central nervous system below excitotoxic levels. In addition to sustaining a secondary-active glutamate transport, EAAT glutamate transporters also function as anion-selective channels. Here, we report a gating process that makes anion channels associated with a neuronal glutamate transporter, EAAT4, permeable to cations and causes a selective increase of the open probability at voltages negative to the actual current reversal potential. The activation process depends on both membrane potential and extracellular glutamate concentration and causes an accumulation of EAAT4 anion channels in a state favoring cation influx and anion efflux. Gating of EAAT4 anion channels thus allows a switch between inhibitory currents in resting cells and excitatory currents in electrically active cells. This transporter-mediated conductance could modify the excitability of Purkinje neurons, providing them with an unprecedented mechanism for adaptation.

anion channel | gating | selectivity | excitatory amino acid transporter

Excitatory amino acid transporters (EAATs) are known to function as glutamate carriers (1–4) and as anion channels (5–8). EAAT-mediated glutamate transport terminates glutamatergic synaptic transmission, ensures low resting extracellular glutamate levels, and prevents neuronal damage by excessive glutamate receptor activation in the mammalian central nervous system. In contrast, the physiological function of EAAT-associated anion currents is not well understood. EAAT-associated anion currents are thought to support electrogenic glutamate uptake by clamping the membrane potential to negative values (6). Additionally, they might also inhibit neuronal excitability by increasing the resting membrane conductance and decreasing length constants of different neuronal compartments (2).

EAAT4 is predominantly expressed in dendritic spines of Purkinje neurons (7, 9, 10). It displays a significant anion conductance (7) and does not play a crucial role in cerebellar glutamate homeostasis (11), suggesting that its major role might be regulation of neuronal excitability as a glutamate-dependent anion channel (2). We studied functional properties of EAAT4 anion channels heterologously expressed in mammalian cells. Our experiments identified a voltage- and glutamate-dependent gating process that changes the selectivity of individual channels and permits EAAT4 anion channels to conduct excitatory currents under certain conditions and inhibitory under others.

Methods

Expression of EAAT4 and Whole-Cell Recordings. Heterologous expression of rEAAT4 in tsA201 cells was performed as described (12). In some of the experiments, a stable inducible cell line, generated by selecting Flp-In-T-Rex 293 cells (Invitrogen) transfected with pcDNA5-FRT-TO-rEAAT4, was used 24 h after incubation with 1 μg/ml tetracycline. Standard whole-cell and outside-out patch clamp recordings were performed by using an EPC10 (HEKA Electronics, Lambrecht, Germany) amplifier (12). Pipettes were pulled from borosilicate glass and had resistances between 1.4 and 2.2 MΩ (1.8 $\pm$ 0.1 MΩ, n = 32). A total of 60–80% of the series resistance was compensated by an analog procedure, so that the calculated voltage error due to access resistance was always <2 mV. The whole-cell resistance under standard conditions was 300 $\pm$ 50 MΩ (n = 32). Pipettes were covered with dental wax to reduce their capacitance. Cells and patches were clamped to the reversal potential for at least 10 s between test sweeps. Standard solutions contained: extracellular, 140 mM $NaNO_3$, 4 mM KCl, 2 mM $CaCl_2$, 1 mM $MgCl_2$, 5 mM Hepes, pH 7.4; intracellular, 115 mM NaCl, 2 mM $MgCl_2$, 5 mM EGTA, 10 mM Hepes, pH 7.4. Unless otherwise stated, 500 μM L-glutamate was added to the external solution. In some experiments, $NaNO_3$ was replaced by NaSCN in the external solution. Under these ionic conditions, untransfected tsA201 cells (12), tsA201 cells expressing a nonfunctional anion channel (L590X hClC-1; ref. 13) or uninduced rEAAT4 Flp-In-T-Rex cells exhibit negligible current amplitudes. Junction potentials were corrected as described (12). The external solution in Fig. 3 contained 150 mM $NaNO_3$, 2 mM $Ca(NO_3)_2$, and 5 mM Hepes, pH 7.4. In the experiments shown in Fig. 3*E*, 20 mM $CaGluconate_2$ was added to this solution. Experiments shown in Fig. 3*D* were performed with cells that were externally perfused with three different solutions containing X $NaNO_3$, 150 mM–X $NMDGNO_3$, 2 mM $Ca(NO_3)_2$, and 5 mM Hepes (pH 7.4). Mes was used to buffer pH 6.0 in Fig. 3*F*. In the experiments shown in Fig. 3*G*, the internal solution was modified by adding 5 mM NaGlutamate or by replacing NaCl by KCl. For Fig. 3*H*, intracellular Cl^- was substituted with NO_3^- and $gluconate^-$. $Gluconate^-$ was shown to remain impermeant during slow activation (data not shown). For the experiments with hClC-Kb, cells were cotransfected with pRcCMV-hClC-Kb and pcDNA3.1-Barttin. The standard extracellular solution contained 140 mM NaCl, 4 mM KCl, 2 mM $CaCl_2$, 1 mM $MgCl_2$, 5 mM Hepes, pH 7.4; the standard intracellular solution contained 115 mM NaCl, 2 mM $MgCl_2$, 5 mM EGTA, 10 mM Hepes, pH 7.4. Cells were held at 0 mV, and current amplitudes were measured at a test step to -20 mV without prepulse and after a 9.6-s prepulse to $+60$ mV, respectively (see Fig. 2*C*).

Data Analysis. Data were analyzed with a combination of PULSE, PULSEFIT, PULSETOOLS (HEKA Electronics), and SIGMAPLOT (Jandel, San Rafael, CA) programs. Current amplitudes were used without subtraction procedure, and all summary data are shown as means $\pm$ SEM. Isochronal current amplitudes were measured 2 ms after the voltage step. Time constants of activation (Fig. 1*D*) were determined by fitting a monoexponential function to the dependence of the isochronal current amplitude

Conflict of interest statement: No conflicts declared.

This paper was submitted directly (Track II) to the PNAS office.

Abbreviation: EAAT, excitatory amino acid transporter.

§To whom correspondence should be addressed. E-mail: fahlke.christoph@mh-hannover.de.

© 2005 by The National Academy of Sciences of the USA

www.pnas.org/cgi/doi/10.1073/pnas.0508837103

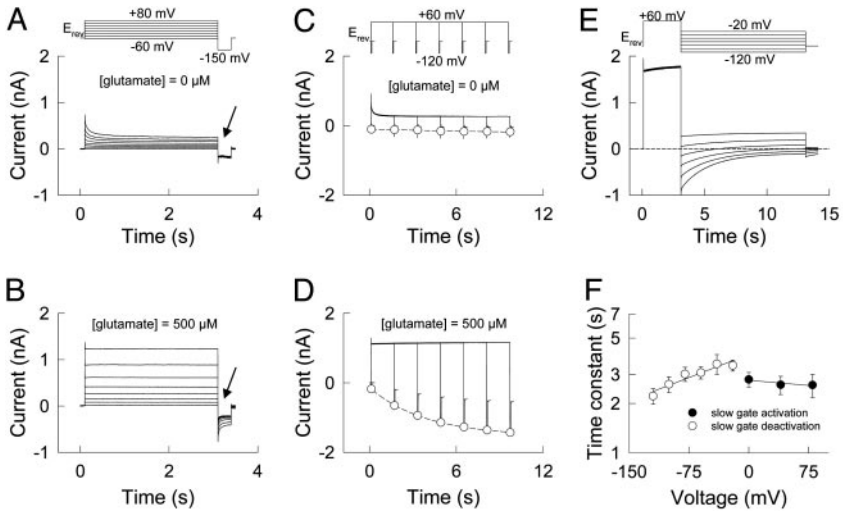

Fig. 1. A gating transition in EAAT4 anion channels during prolonged membrane depolarizations. (*A* and *B*) Representative current recordings in the absence (*A*) or presence (*B*) of glutamate. (*C* and *D*) Current responses to voltage steps to +60 mV of increasing durations followed by fixed test steps to −120 mV. Isochronal tail current amplitudes are represented by symbols and fits with monoexponential functions by dashed lines. (*E*) Current deactivation during hyperpolarizing voltage steps after a depolarizing prepulse. The dashed line gives zero current. (*F*) Voltage dependence of activation and deactivation time constants (means ± SEM, $n = 4$–5).

measured at −120 mV on the length of the preceding membrane depolarization. The time course of slow gate deactivation (Fig. 1*E*) was measured at various negative potentials after a 3-s prepulse to +60 mV to open the gate. Permeability ratios were calculated from reversal potential measurements by using the Goldman–Hodgkin–Katz (GHK) equation (14). Long depolarizations cause small changes of the intracellular anion concentration that need to be taken into account in the quantitative analysis of slow-gating-induced alteration of EAAT4 anion channel selectivity. We calculated changes of the internal $[NO_3^-]$ from the measured NO_3^- influx by using Eq. **3** (see *Supporting Text* and Fig. 5, which are published as supporting information on the PNAS web site) and inserted these values into the GHK equation. For nonstationary noise analysis (see Fig. 4), a series of 300 records was recorded by pulsing to a certain voltage from the holding potential of −60 or 0 mV. Pairs of subsequent records were then subtracted to compute the ensemble variance (15). Background noise was measured at the end of the experiment after taking the pipette out of the bath and subtracted from the ensemble variances. After normalization to the value determined at −180 mV following a holding potential of +60 mV, the square root of the ensemble variances was calculated and plotted versus the normalized mean current amplitudes. Current traces were sampled at 200 kHz and filtered by using a Butterworth low-pass filter with a cutoff frequency of 10 kHz. For all experiments, the analysis was repeated after digital filtering at 5 and 2 kHz with similar results. For all statistic evaluations, Student's *t* test with $P < 0.05$ as level of significance was used.

Results

Voltage-Dependent Activation of EAAT4 Anion Channels. We expressed EAAT4 glutamate transporters heterologously in tsA201 cells and measured currents through whole-cell patch clamp experiments. The so-determined whole-cell currents are pure anion currents, as substitution of internal and external anions with gluconate results in current amplitudes comparable to background currents in nontransfected cells (Fig. 6, which is published as supporting information on the PNAS web site). EAAT4 anion channels are active with or without external glutamate; however, application of substrate increases the current amplitudes and modifies voltage-dependent gating (12) (Fig. 1). In the presence of glutamate, positive voltages cause a pronounced increase of currents at a consecutive test step to a negative potential (Fig. 1*B*, arrow). Gradually incrementing the

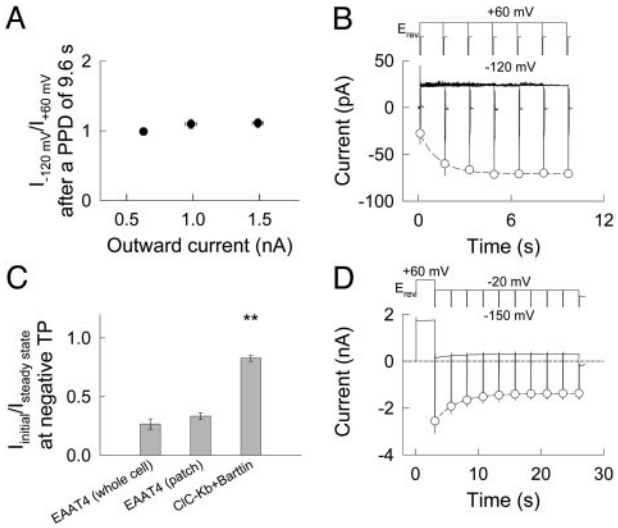

Fig. 2. Enhanced EAAT4 inward currents are not due to anion accumulation. (*A*) Isochronal tail current amplitudes at −120 mV after a 9.6-s prepulse normalized to the prepulse current amplitude from current responses to the pulse protocol shown in Fig. 1*C*. Data from 30 cells expressing different levels of EAAT4 were binned into three data groups that were statistically not different. (*B*) Current responses to voltage steps to +60 mV of increasing durations followed by fixed test steps to −120 mV in an outside-out patch from cells expressing EAAT4 transporters. Isochronal tail current amplitudes are represented by symbols and fits with monoexponential functions by a dashed line. The patch was clamped to −23 mV between test sweeps. Because of the larger contribution of leak current in outside-out patches, this value is more positive than reversal potentials in whole-cell experiments (−61.9 ± 0.9 mV, $n = 32$). (*C*) Ratio of the tail current amplitudes after stepping from the holding potential by the corresponding value after a prepulse of 9.6 s from current responses to the pulse protocol shown in *B*. Means ± SEM from cells ($n = 19$) and patches ($n = 5$) expressing EAAT4 and cells expressing hClC-Kb and barttin ($n = 4$), respectively, are shown. **, Significant difference to EAAT4 at $P < 0.01$. (*D*) EAAT4 anion channel deactivation at potentials positive to the anion reversal potential. After an activating prepulse to +60 mV, the cell was clamped to −20 mV, and fixed test steps to −150 mV were applied every 2.5 s.

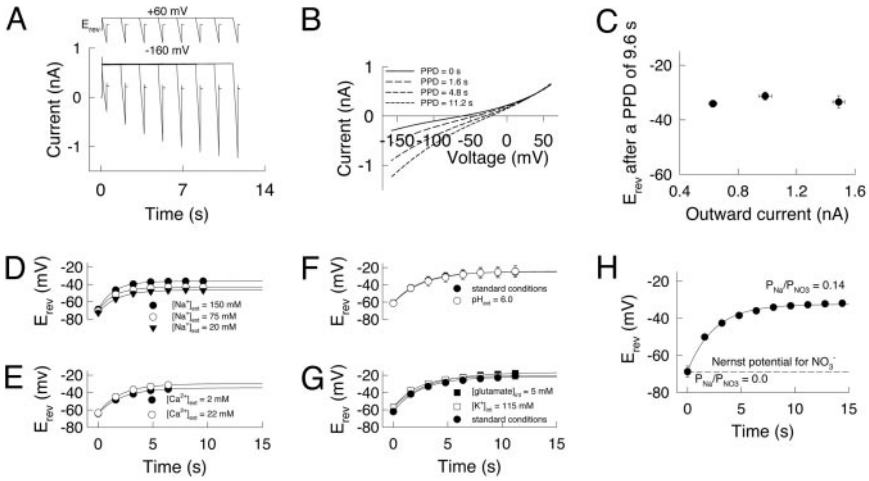

Fig. 3. Activation of the slow gate is associated with increasing cation permeabilities of EAAT4 channels. (*A*) Current responses to voltage ramps after prepulses of variable duration. (*B*) Voltage dependence of the current amplitudes recorded during voltage ramps before and after different prepulse durations (PPD) from the experiment shown in *A*. (*C*) Plot of the corrected steady state reversal potential versus the outward current amplitude at +60 mV. Data from 30 cells were binned into three data groups that were statistically not different. (*D*) Time course of current reversal potentials determined from voltage ramp experiments on four cells with different external $[Na^+]_o$. (*E*) Time course of current reversal potentials determined from voltage ramp experiments on four cells with different external $[Ca^{2+}]_o$. (*F*) Time course of current reversal potentials determined from four cells perfused with standard solutions with pH 7.4 (filled circles) and consequently with pH 6.0 (open circles). (*G*) Reversal potentials from cells under standard conditions (filled circles, $n = 14$), cells dialyzed with an internal solution containing 5 mM glutamate (filled squares, $n = 2$), and cells dialyzed with an internal solution in which Na^+ was completely replaced by K^+ (open squares, $n = 4$). (*H*) Time course of current reversal potential using an internal solution containing 10 mM $NaNO_3$ and 100 mM NaGluconate. All reversal potentials are given as means ± SEM.

length of a depolarizing prepulse evokes a time-dependent increase of the current amplitude at a successive test step to −120 mV, whereas the amplitude at positive potentials remains basically unaltered (Fig. 1*D*). Without glutamate, there is only a small, if any, enhancement of the tail current amplitudes (Fig. 1 *A*, arrow, and *C*). The time course of activation (Fig. 1*D*) as well as the time course of deactivation during membrane hyperpolarization after a long activating prepulse (Fig. 1*E*) displays time constants in the range of seconds (Fig. 1*F*). Deactivation time constants depend on extracellular glutamate: when measured in a stream of glutamate-free solution after activation in a glutamate-containing solution, they are markedly slower [τ_{deact} (−80 mV) = 6.9 ± 0.5 s, $n = 4$] than those determined in the presence of glutamate (3.3 ± 0.4 s, $n = 5$).

A possible artifactual explanation for the observed changes of inward current amplitudes was that NO_3^- entering the cell during depolarization accumulated inside the cell and carried the inward current upon repolarization. We designed several experiments to test this possibility. In case of pure anion accumulation, the increases of the tail current amplitudes in pulse protocols such as in Fig. 1*D* should depend on the magnitude of anion influx and thus on the expression levels of the channel. In contrast to this prediction, a comparison between cells expressing different EAAT4 levels (Fig. 2*A*) revealed that the ratios of tail current by prepulse current amplitude do not change for anion influx current amplitudes between 200 pA and 2 nA. Moreover, slow activation of EAAT4 anion channel depends on glutamate (Fig. 1). If the time- and voltage-dependent increase of the tail current amplitudes were solely caused by changes of the intracellular anion concentration, equal amounts of anions entering the cell would result in identical tail current amplitudes, regardless of the external glutamate concentration. However, in the absence of glutamate, similar time-dependent anion current increases were never observed, not even in cells with expression levels that result in large current amplitudes under these conditions (data not shown). EAAT4 anion currents are small when studied in excised outside-out patches (53 ± 19 pA, $n = 5$, at +60 mV), so that anion accumulation in the internal solution is virtually impossible. However, the typical prepulse-induced increases of the inward current could be also observed in this recording mode (Fig. 2*B*). The time constants (2.5 ± 0.9 s, $n = 5$, at +60 mV) and the magnitude of the depolarization-induced enhancement of inward currents were similar in patches and in whole-cell measurements (Figs. 1*F* and 2*C*). We performed additional whole-cell experiments with another type of anion channel, hClC-Kb, together with its accessory subunit Barttin (Fig. 2*C*) (16). Although the anion influx into these cells during the prepulse (current amplitude at +60 mV 1.1 ± 0.3 nA, $n = 5$) was comparable to experiments with EAAT4 (1.3 ± 0.2 nA, $n = 8$), application of depolarizing prepulses of increasing durations resulted in only small time-dependent enhancements of the tail current amplitudes. If the increase of the after-depolarization inward current were caused by intracellular anion accumulation, identical anion influxes should result in similar enhancements of the tail current amplitude independently of the underlying anion channel. Another argument stems from the voltage dependence of channel deactivation. If anion accumulation were the sole basis of the observed changes in current amplitude, the current decay at negative potentials must be caused by an outward movement of anions and is therefore only possible at voltages negative to the anion reversal potential. However, application of a potential positive to the anion reversal potential (−20 mV) after a prepulse to +60 mV causes a decrease of tail current amplitudes at test steps to −150 mV (Fig. 2*D*). Taken together, these lines of evidence refute anion accumulation as the sole basis of the observed changes of EAAT4 anion current amplitudes and establish the existence of a previously uncharacterized gating process, designated slow activation.

The experiments described so far were performed under nonphysiological ionic conditions using voltage protocols that do not resemble the electrical activity of Purkinje neurons. However, slow activation also occurs under an approximately physiological anion gradient with $[Cl^-]_i$ of 10 mM and $[Cl^-]_o$ of 150 mM (data not shown), and with K^+ as the main internal cation (Fig. 3*G*). The slow gate is activated not only by long tonic depolarizations, but also by a series of phasic depolarizations (see *Supporting Text* and Fig. 7, which is published as supporting

information on the PNAS web site). These results, taken together, demonstrate that slow gating can occur in native Purkinje cells under physiological conditions.

Slow Gating Increases Cation Permeability of EAAT4 Anion Channels. To study slow gating-induced changes of EAAT4 channels in more detail, we applied voltage ramps after depolarizing prepulses of variable durations (Fig. 3*A*). Fig. 3*B* shows the voltage dependence of EAAT4 currents obtained from these pulse protocols. Depolarizing prepulses decrease outward and increase inward currents and shift the current reversal potential more positive indicating a time- and voltage-dependent variation of the selectivity of EAAT4 anion channels. The changes of the current reversal potential do not depend on the magnitude of anion influx (Fig. 3*C*), providing an additional argument against anion accumulation. The shift of ion selectivity can be directly demonstrated by applying hyperpolarizing voltage steps of −60 mV or −80 mV after a depolarizing prepulse. Under these conditions, the initial inward current decreases in amplitude and then reverses to an outward current (Fig. 1*E*).

To define the particular ions whose permeabilities change during slow activation, we performed ion substitution experiments. Cells were moved in the streams of different external solutions, and current reversal potentials were determined from voltage ramps after various durations of a prepulse to +60 mV. Reversal potentials were then plotted versus the prepulse duration (Fig. 3 *D–H*), demonstrating that channel selectivity changes with the same time course as current amplitudes in Fig. 1*D*. Changing external $[Na^+]$ (Fig. 3*D*) or external $[Ca^{2+}]$ (Fig. 3*E*) affected the steady-state reversal potentials, but left the initial values unaffected, indicating that Na^+ and Ca^{2+} become permeant during slow activation. Neither protons nor glutamate are permeant under any tested condition (Fig. 3 *F* and *G*). Activated EAAT4 channels do not select between monovalent cations, as intracellular substitution of Na^+ by K^+ does not modify current reversal potentials (Fig. 3*G*). To determine the cation to anion permeability ratio, experiments were performed with only one permeant anion, NO_3^-, on both sides of the membrane (Fig. 3*H*). After deactivation of the slow gate, EAAT4 currents reverse at the predicted anion reversal potential, indicating ideal anion selectivity. Depolarizing prepulses result in reversal potentials that correspond to a P_{Na}/P_{NO3} of 0.14 ± 0.02 (n = 4). Using the NO_3^- to Cl^- permeability ratio determined from reversal potentials in the slow deactivated state (P_{NO3}/P_{Cl} = 9.4 ± 0.4; n = 30) and assuming that there is no change of the relative anion selectivity due to slow gate activation, these two values result in a P_{Na}/P_{Cl} permeability ratio of 1.3 ± 0.2. A P_{Ca}/P_{Cl} of 1.7 ± 0.2 (n = 4) was calculated from the measured steady state reversal potentials upon elevated $[Ca^{2+}]_o$ (Fig. 3*E*). These results demonstrate that, with Cl^- as the main anion, monovalent and divalent cations are considerably permeant through EAAT4 anion channels in the slow-activated state.

Cations could permeate the same ion conduction pathway as anions, or, alternatively, slow gating could open additional cation-permeable pores. We used noise analysis to distinguish between these two possibilities (17). EAAT4 anion channels produce a Lorentzian noise that can be measured by whole-cell recordings (Fig. 4*A*) (see *Supporting Text*). At the current reversal potential, the unitary current amplitudes of a pore permeable to both anions and cations are zero. Therefore, current variances, determined before and after slow activation at the respective reversal potentials, will be identical for this scenario. In contrast, in case of separate anion- and cation-conducting pores, each pore would fluctuate between zero and nonzero current amplitudes, resulting in an increased current variance at the apparent reversal potential after slow activation. We determined current variances at two different potentials: at −27 mV, the potential at which currents reverse on average after an activating prepulse to 0 mV, and at −61 mV, the reversal potential after a prepulse to −60 mV, respectively. The two current variances are not significantly different (σ^2 = 45 ± 8 pA^2 and σ^2 = 41 ± 9 pA^2, n = 8) indicating that slow activation modifies the cation to anion selectivity of a single ion conduction pathway of EAAT4 anion channels (17). Cation currents are nonexistent in the absence of permeant anions (Fig. 6), indicating that cations can only permeate through this ion conduction pathway together with anions.

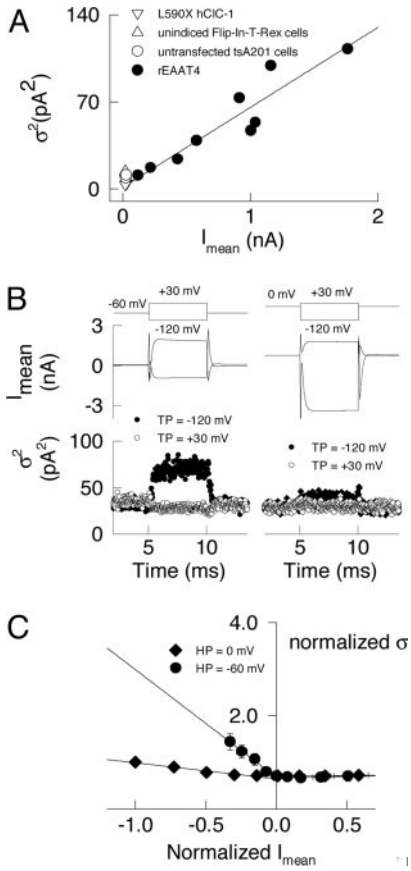

Fig. 4. Activation of the slow gate increases the open probability of the EAAT4 anion channels. (*A*) Plot of the current variance at −120 mV versus the mean current amplitude determined from nine tsA201 cells transiently transfected with cDNA encoding for EAAT4 transporters (filled circles), four tsA201 cells transiently transfected with cDNA encoding for a nonconducting hClC-1 mutant (L590X hClC-1, open inverted triangles), five untransfected tsA201 cells (open circles), and four uninduced Flp-In T-Rex HEK293 cells (open triangles). The correlation coefficient between both parameters in rEAAT4-transfected cells is r = 0.93. (*B*) Time course of mean currents and variances measured at test potentials of −120 mV (filled symbols) and +30 mV (open symbols) stepping from holding potentials of −60 and 0 mV. The external solution contained NaSCN. (*C*) Plot of the normalized isochronal current standard deviation versus the normalized mean current amplitude, determined at test steps to potentials between −180 and 60 mV from holding potentials of −60 mV (filled circles) and 0 mV (filled diamonds) (means ± SEM, n = 8), respectively.

Slow Gating Alters the Open Probability of EAAT4 Anion Channels Depending on the Current Direction. Ion substitution experiments demonstrated that slow gating functionally changes the anion conduction pathway of EAAT4. To test whether it also modifies the open probability, i.e., the proportion of time the EAAT4 anion channel is conducting anions, we used a variation of nonstationary noise analysis. We determined isochronal standard deviations 2 ms after steps to various voltages from holding potentials of −60 and 0 mV, respectively (Fig. 4 *B* and *C*) and

plotted them versus the mean current amplitude. For such a plot, the slope of a linear regression depends on the absolute open probability $p(V)$ and the number of channels N

$$\sigma(V) = I(V)\sqrt{\frac{\frac{1}{p(V)} - 1}{N}}$$

(18) (see *Supporting Text*), i.e., an increased absolute open probability results in a less steep relationship between standard deviation and current amplitude. For both holding potentials, the plots can be well described with two lines having different slopes at positive and at negative current amplitudes, demonstrating that the absolute open probability after a prescribed prepulse can assume two different values, one at potentials positive and another one at potentials negative to the current reversal potential. For EAAT4 anion channels, a holding potential of 0 mV causes an isolated increase of the open probability at potentials negative the current reversal potential, but leaves current amplitudes and current variances at positive potentials virtually unaffected. Thus, slow activation increases only the number of open channels permitting an inward current, but not of those conducting an outward current.

Discussion

EAAT4 transporters are known to mediate three different transport processes. They function as secondary-active glutamate transporters and as anion-selective ion channels. Additionally, they display a glutamate- and arachidonic acid-activated proton conductance (19). Here, we report that the selectivity of EAAT4 anion channels can be changed from ideally anion-selective to partially cation-permeable by a glutamate- and voltage-dependent gating process. Inward and outward anion currents are independently gated (Fig. 4*C*), allowing a selective modification of the inward current amplitude without affecting outward currents. Slow gating does not modify the proton permeability (Fig. 3*G*), indicating that the EAAT4 proton channel is not controlled by the slow gate.

The two unique qualities of the associated anion channel give EAAT4 transporters the remarkable ability to either inhibit or excitate neuronal cells, depending on conditions and history. Under resting conditions, EAAT4 anion channels are ideally anion-selective and thus inhibit cell excitability. Trains of phasic depolarizations and long-lasting depolarizations (20, 21) cause slow activation and change the number and selectivity of open channels. Because deactivation is extremely slow, Purkinje cell excitation is followed by an excitatory inward current of several seconds through slow activated EAAT4 channels.

EAAT4 transporters are primarily expressed in spines of Purkinje dendrites (10), precluding a detailed analysis of slow gating in native tissue. However, functional properties of EAAT4 anion channels in heterologous expression systems are very similar to those found in native cells (22). Thus, the reported slow-gating induced changes of EAAT4 currents, together with EAAT4 densities in spines (10, 22) and estimates of passive electric properties of these neuronal compartments, allow an approximation of slow activation-induced changes of the spinal membrane potential (see *Supporting Text*). Spines in Purkinje cell dendrites are small units with a high input resistance (23), and the estimated EAAT4 inward cation current will depolarize the spine membrane potential by ≈25 mV (see *Supporting Text*). Because Ca^{2+} influx through activated EAAT4 channels potentially modifies Ca^{2+} release from intracellular stores (24), EAAT4 anion channels might also play a role in neuronal plasticity (24, 25). The unusual features of slow activation thus allow EAAT4 to modify excitability, firing frequency, and Ca^{2+} signaling in Purkinje neurons.

In all known ion channels involved in electrical signaling, changes in open probability modify the membrane conductance for permeant ions over the whole voltage range. In such cases, the effect of channel activation on the membrane potential depends on the ion concentration on both sides and is therefore, in most cases, an invariable property of the channel. EAAT4 transporter-associated anion channels exhibit a totally novel behavior. They conduct inhibitory as well as excitatory currents, and they switch between inhibitory and excitatory action in short periods of time, without requiring energetically costly alterations of bulk solution ion concentrations. Slow gating of EAAT4 anion channels most likely obtains its glutamate and voltage dependence from the association to the glutamate carrier. The gating process defines a likely physiological role of EAAT4 transporter-associated ion channels and demonstrates the impact of the tight coupling of anion channel and glutamate carrier in this class of membrane proteins.

We thank Drs. A.L. George (Vanderbilt University, Nashville, TN), D. Naranjo (Centro de Neurociencias de Valparaiso, Universidad de Valparaiso, Valparaiso, Chile), and J. Rothstein (John Hopkins University, Baltimore) for providing the expression construct for hClC-Kb, barttin, F425GΔ6–46 *Shaker*, and rEAAT4, respectively; Drs. Louis DeFelice, Patricia Hidalgo, J. P. Johnson, Günther Schmalzing, and the participants of the Ion Channel Carnival (December 2004, Valdivia, Chile) for helpful discussions; and Hannelore Heidtmann and Barbara Poser for excellent technical assistance. These studies were supported by the Deutsche Forschungsgemeinschaft [FOR450, TP4 (to Ch.F.)] and Studienstiftung des Deutschen Volkes (to N.M.).

1. Danbolt, N. C. (2001) *Prog. Neurobiol.* **65,** 1–105.
2. Amara, S. G. & Fontana, A. C. (2002) *Neurochem. Int.* **41,** 313–318.
3. Kanner, B. I. (1996) *Biochem. Soc Trans.* **24,** 843–846.
4. Billups, B., Rossi, D., Oshima, T., Warr, O., Takahashi, M., Sarantis, M., Szatkowski, M. & Attwell, D. (1998) *Prog. Brain Res.* **116,** 45–57.
5. Larsson, H. P., Picaud, S. A., Werblin, F. S. & Lecar, H. (1996) *Biophys. J.* **70,** 733–742.
6. Wadiche, J. I., Amara, S. G. & Kavanaugh, M. P. (1995) *Neuron* **15,** 721–728.
7. Fairman, W. A., Vandenberg, R. J., Arriza, J. L., Kavanaugh, M. P. & Amara, S. G. (1995) *Nature* **375,** 599–603.
8. Billups, B., Rossi, D. & Attwell, D. (1996) *J. Neurosci.* **16,** 6722–6731.
9. Yamada, K., Watanabe, M., Shibata, T., Tanaka, K., Wada, K. & Inoue, Y. (1996) *NeuroReport* **7,** 2013–2017.
10. Dehnes, Y., Chaudhry, F. A., Ullensvang, K., Lehre, K. P., Storm-Mathisen, J. & Danbolt, N. C. (1998) *J. Neurosci.* **18,** 3606–3619.
11. Huang, Y. H., Dykes-Hoberg, M., Tanaka, K., Rothstein, J. D. & Bergles, D. E. (2004) *J. Neurosci.* **24,** 103–111.
12. Melzer, N., Biela, A. & Fahlke, Ch. (2003) *J. Biol. Chem.* **278**, 50112–50119.
13. Hebeisen, S., Biela, A., Giese, B., Muller-Newen, G., Hidalgo, P. & Fahlke, Ch. (2004) *J. Biol. Chem.* **279**, 13140–13147.
14. Lewis, C. A. (1979) *J. Physiol. (London)* **286,** 417–445.
15. Heinemann, S. H. & Conti, F. (1992) *Method Enzymol.* **207,** 131–148.
16. Estevez, R., Boettger, T., Stein, V., Birkenhager, R., Otto, E., Hildebrandt, F. & Jentsch, T. J. (2001) *Nature* **414,** 558–561.
17. Dionne, V. E. & Ruff, R. L. (1977) *Nature* **266,** 263–265.
18. Hebeisen, S., Heidtmann, L., Cosmelli, D., Gonzalez, C., Poser, B., Latorre, R., Alvarez, O. & Fahlke, Ch. (2003) *Biophys. J.* **84**, 2306–2318.
19. Fairman, W. A., Sonders, M. S., Murdoch, G. H. & Amara, S. G. (1998) *Nat. Neurosci.* **1,** 105–113.
20. Canepari, M., Auger, C. & Ogden, D. (2004) *J. Neurosci.* **24,** 3563–3573.
21. Tempia, F., Alojado, M. E., Strata, P. & Knopfel, T. (2001) *J. Neurophysiol.* **86,** 1389–1397.
22. Otis, T. S., Kavanaugh, M. P. & Jahr, C. E. (1997) *Science* **277,** 1515–1518.
23. Rapp, M., Segev, I. & Yarom, Y. (1994) *J. Physiol. (London)* **474,** 101–118.
24. Berridge, M. J. (1998) *Neuron* **21,** 13–26.
25. Sabatini, B. L., Maravall, M. & Svoboda, K. (2001) *Curr. Opin. Neurobiol.* **11,** 349–356.

Supporting Text

Time-Dependent Changes of the Intracellular Anion Composition. The long depolarizations necessary to activate the slow gate (Fig. 1) might cause changes of the intracellular anion composition that could contribute to the time-dependent changes of the current amplitude and affect the accuracy in determining relative cation to anion permeabilities. Changes of the intracellular anion concentration (c_i) of a cell in the whole-cell mode at a constant anion influx (j) depend on the volume of the cell V_i, the series resistance R_s, the diffusion coefficient D and the resistivity ρ of the intracellular solution (1 - 3). c_p denotes the anion concentration in the pipette.

$$\frac{dc_i}{dt} = \frac{1}{V_i} j - \frac{1}{\tau_p}(c_p - c_i) \qquad [1]$$

with τ_p given by

$$\tau_p = \frac{R_s V_i}{D\rho} \qquad [2]$$

This equation can be solved when the anion flux j across the membrane is constant.

$$c_i(t) = c_i(0) + \frac{j}{V_i}\tau_p(1 - e^{-\frac{t}{\tau_p}}) \qquad [3]$$

In our experiments, τ_p is ≈ 60 s, based on average values of the series resistance R_s (≈ 4 MΩ, ref. 3), the cell volume V_i (≈ 20 x 10^{-15} m^3, calculated from reported tsA201 capacitances, ref. 4) the diffusion coefficient D (19 x 10^{-10} m^2/s for NO_3^-, ref. 5) and the resistivity ρ (0.7 Ωm, ref. 6) of the intracellular solution. The calculated time constant is ≈ 20 times larger than the activation and deactivation time constants of slow gating (Fig. 1*F*) and

thus represents an additional argument against anion accumulation as the sole basis of the observed changes of the inward current and reversal potential.

The analysis does predict small changes of the intracellular anion concentration that need to be taken into account in the quantitative analysis of slow-gating induced alteration of EAAT4 anion channel selectivity. Based on the anion current amplitude during the depolarizing prepulse, we calculated changes of the internal anion concentration and corrected the measured reversal potential for this value (Fig. 5). This correction resulted in an average subtraction of 7.5 ± 0.5 mV (n = 30) from the steady state reversal potential. Fig. 3*C* gives the plot of corrected current reversal potentials determined at different cells versus the EAAT4 current amplitudes. There is no dependence of the reversal potentials on the current amplitude demonstrating that the correction is adequate and that the corrected values allow an accurate determination of anion to cation permeability ratios.

Trains of Phasic Depolarizations Cause Slow Activation. Application of repetitive short voltage steps of different frequencies, followed by a fixed 10s test step to –80 mV, cause a time and frequency-dependent increase of the tail current amplitude (Fig. 7). Increasing the frequency of the transient depolarizations (Fig. 7 *A* and *B*) augmented the current amplitudes at negative, but not at positive potentials. Fig. 7*C* gives a plot of the instantaneous tail current amplitude at –80 mV (arrows in Fig. 7*A* and *B*) charted against several excitation frequencies. Within a frequency range typical of spontaneous burst firing of Purkinje cell dendrites (7, 8), current amplitudes at negative potentials increase threefold.

The Observed Current Variance Is EAAT4 Channel-Associated Noise. We determined current variances in transfected tsA201 cells, as well as in untransfected tsA201 cells, tsA201 cells expressing a non-functional anion channel (L590X hClC-1, ref. 9), and in uninduced

rEAAT4 Flp-In-T-Rex cells. For tsA201 cells expressing EAAT4, we observed a clear correlation between EAAT4 current levels and current variance (r = 0.93), while untransfected and uninduced cells, as well as cells expressing large quantities of a non-conducting membrane protein (9) have markedly reduced current variances (Fig. 4 *A*). Moreover, in cells that do not express EAAT4, the current variance at a test potential of –120 mV is independent from the holding potential (data not shown). These results demonstrate that the current variance measured in transfected cells is caused by EAAT4 channels and not by endogenous ion channels. Increased current amplitudes at negative test potentials after depolarizing prepulses are associated with reduced current variances (Fig. 4), demonstrating that the measured current variance is not thermal noise associated with the recording pipettes, shunt resistances, membrane impedances or electrical circuits, but rather Lorentzian noise associated with gating of EAAT4-associated channels.

To study slow gating induced changes of the open probability of EAAT4-associated anion channels, the current standard deviation was determined as the square root of the non-stationary noise measured 2 ms after the voltage step for various voltages and plotted versus the mean current amplitudes determined at the same time (Fig. 4 *B* and *C)*. Lorentzian noise depends on the number of channels (*N*), the unitary current amplitude (*i*) and the absolute open probability (*p*). The measured variance is equal to:

$$\sigma^2(V) = Ni^2(V)\, p(V)\, (1 - p(V)) + \sigma_0^2 \qquad [4]$$

with σ_0^2 being the background noise.

In this experiment, the unitary current amplitude is not constant and substitution of

$$i(V) = \frac{I(V)}{Np(V)} \qquad [5]$$

into Eq. 4 yields:

$$\sigma^2 = \frac{I^2(V)}{N}\left(\frac{1}{p(V)} - 1\right) + \sigma_0^2 \qquad [6]$$

After subtraction of the background noise, Eq. 6 can be transformed to Eq. 7:

$$\sigma_{app} = \sqrt{\sigma^2 - \sigma_0^2} = I(V)\sqrt{\frac{\frac{1}{p(V)} - 1}{N}} \qquad [7]$$

This analysis shows that the slope of a straight line fitted to the standard deviation-mean current plot solely depends on the open probability and that the observed change of the slope by a depolarizing prepulse (Fig. 4*C*) is due to a change of the open probability of EAAT4 channels. Control experiments with voltage-gated potassium channels (10) provide identical open probabilities for inward and outward currents (Fig. 8), demonstrating that this behavior is specific for glutamate transporter-associated channels.

Approximation of EAAT4 Current Amplitudes and Resulting Voltage Changes in Spines of Purkinje Cell Dendrites. Published values (11) of the EAAT4 transporter density, their distribution and the mean spine surface area (12) predict ≈ 4900 transporters per spine that are in direct vicinity to the presynaptic glutamate release sites and thus face synaptically released glutamate. Transporters in the dendritic membrane adjacent to the spine were not included in our analysis.

A single channel amplitude of 25 fA in external NO_3^- in the presence of glutamate at 0 mV was calculated using published unitary current amplitudes (13). This value was then used to scale the current-voltage relationships shown in Fig 3*B*. The so-obtained voltage dependence of unitary, slow activated EAAT4 current amplitudes was multiplied by the number of transporters in a single synaptic spine and the absolute open probability resulting in a total spine current amplitude of about 175 pA at –60 mV (14) carried entirely by slowly activated EAAT4 transporters. Assuming an input resistance of a single spine R_{in} = 400 MΩ

(14), this current flow gives rise to a membrane depolarization of ≈ 25 mV, demonstrating a physiological relevance of slow activation of EAAT4 inward currents in synaptic transmission.

1. Oliva, C., Cohen, I. S. & Mathias, R. T. (1988) *Biophys. J.* **54**, 791-799.
2. Mathias, R. T., Cohen, I. S. & Oliva, C. (1990) *Biophys. J.* **58**, 759-770.
3. Marty, A. & Neher, E. (1995) in *Single-Channel Recording*, eds. Sakmann, B. & Neher, E. (Plenum, New York), pp. 31-52.
4. Santos-Sacchi, J., Shen, W., Zheng, J. & Dallos, P. (2001) *J. Physiol. (London)* **531**, 661-666.
5. Hille, B. (1992) *Ionic Channels of Excitable Membranes* (Sinauer, Sunderland, MA).
6. DeFelice, L. J. (1981) in *Introduction to Membrane Noise* (Plenum, New York), pp. 115-230.
7. Llinas, R. & Sugimori, M. (1980) *J. Physiol. (London)* **305**, 171-195.
8. Llinas, R. & Sugimori, M. (1980) *J. Physiol. (London)* **305**, 197-213.
9. Hebeisen, S., Biela, A., Giese, B., Müller-Newen, G., Hidalgo, P. & Fahlke, Ch. (2004) *J. Biol. Chem.* **279**, 13140-13147.
10. Goldstein, S. A., Pheasant, D. J. & Miller, C. (1994) *Neuron* **12**, 1377-1388.
11. Takahashi, M., Sarantis, M. & Attwell, D. (1996) *J. Physiol. (London)* **497**, 523-530.
12. Dehnes, Y., Chaudhry, F. A., Ullensvang, K., Lehre, K. P., Storm-Mathisen, J. & Danbolt, N. C. (1998) *J. Neurosci.* **18**, 3606-3619.
13. Melzer, N., Biela, A. & Fahlke, Ch. (2003) *J. Biol. Chem.* **278**, 50112-50119.
14. Rapp, M., Segev, I. & Yarom, Y. (1994) *J. Physiol. (London)* **474**, 101-118.

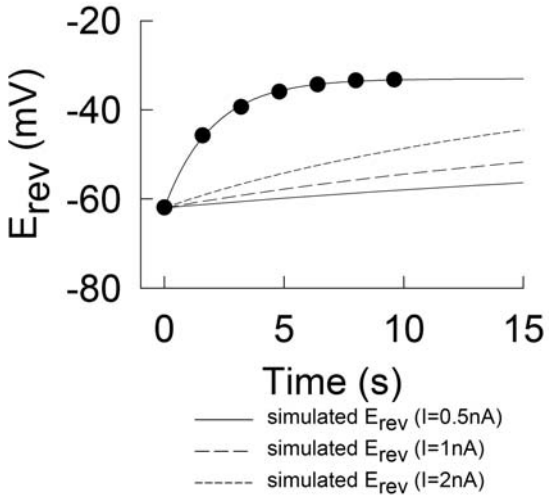

Fig. 5. Slow gating-induced alterations of the reversal potentials are much larger than those predicted for anion accumulation. Time course of the simulated reversal potential shift caused by alteration of the intracellular anion composition due to anion influx of 0.5 nA (solid line), 1 nA (long dashed line), and 2 nA (short dashed line) and measured means ± SEM of the reversal potential (filled circle) from cells with inward current amplitudes between 0.5 and 2 nA.

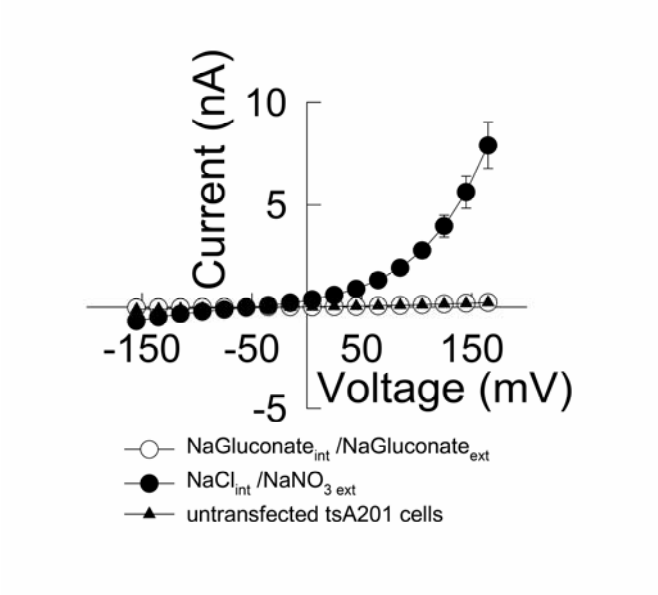

Fig. 6. Whole-cell currents in EAAT4-expressing cells represent glutamate transporter-associated anion currents. Current-voltage relationships of EAAT4 whole-cell currents under standard conditions (filled circle) and in the absence of permeant anions (open circle), and of whole-cell currents of untransfected cells under standard conditions (filled triangle). Means ± SEM, $n > 4$.

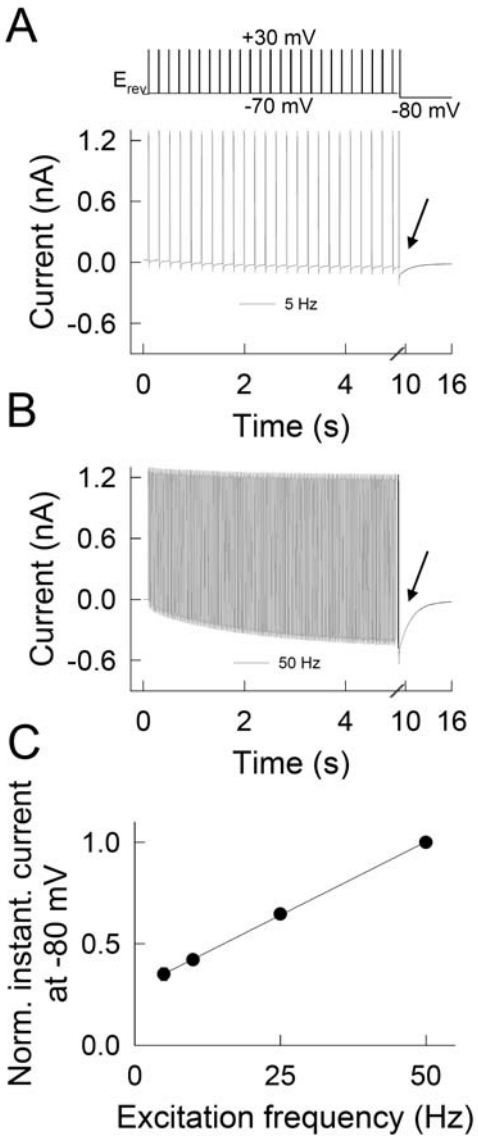

Fig. 7. Slow activation during repetitive short depolarizations. (*A* and *B*) Current responses to repetitive depolarizations at frequencies of 5 Hz (*A*) and 50 Hz (*B*) followed by a fixed test step to **-**80 mV. The cell was perfused with a NaSCN-based solution. (*C*) Frequency dependence of the normalized isochronal tail current amplitude (arrows) (means ± SEM, n = 5).

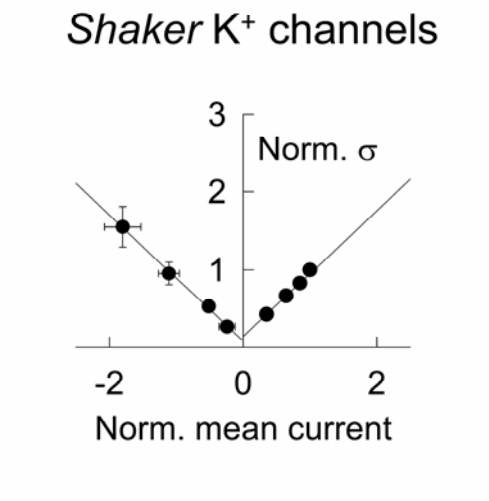

Fig. 8. Plot of normalized isochronal current standard deviations versus normalized mean current amplitudes of F425G *Shaker* potassium channels (means ± SEM, n = 6). tsA201 cells were transfected with pMTO3-F425G *Shaker* K+ channels and studied by using whole-cell patch clamp recordings with an internal solution containing 120 mM KCl, 2 mM $MgCl_2$, 5 mM EGTA, 10 mM Hepes, pH 7.4, and an external solution of 144 mM KCl, 2 mM $CaCl_2$, 1 mM $MgCl_2$, 5 mM Hepes, pH 7.4. Cells were held at -80 mV, channels were activated at 0 mV for 3 ms, and isochronal currents and standard deviations were determined 1 ms after stepping to various voltages.

Zusammenfassung

Einleitung

Der Neurotransmitter Glutamat wird nach seiner Freisetzung aus dem präsynaptischen Neuron durch spezielle Glutamattransporter aus dem synaptischen Spalt in benachbarte Glia-Zellen und das prä- und postsynaptische Neuron aufgenommen. Diese Glutamattransporter sind Mitglieder der SLC1-Familie sekundär-aktiver Transporter und werden als „Excitatory Amino Acid Transporters“ (EAATs) bezeichnet. Sie vermitteln einen stöchiometrisch gekoppelten und elektrogenen Carriertransportprozeß, in dem ein Glutamatmolekül zusammen mit drei Na^+-Ionen und einem H^+-Ion im Austausch gegen ein K^+-Ion aufgenommen wird. In einem Transportzyklus werden daher zwei positive Nettoladungen in die Zelle hineintransportiert. Der resultierende elektrische Glutamataufnahmestrom hängt von der Anwesenheit intrazellulärer K^+-Ionen ab, da nur so ein vollständiger Transportzyklus durchlaufen werden kann. Dieser Glutamataufnahmeprozeß beendet die glutamaterge Neurotransmission und verhindert die Diffusion des Neurotransmitters zu benachbarten Synapsen. Er sorgt so für die zeitliche und räumliche Begrenzung der synaptischen Übertragung. Weiterhin verhindert die Glutamataufnahme die Akkumulation des Glutamats im synaptischen Spalt und die damit verbundene prolongierte neurotoxische Aktivierung postsynaptischer Glutamatrezeptoren.

Alle fünf bisher bekannten EAAT-Isoformen (EAAT1-5) besitzen neben dem Carrier, der den Glutamataufnahmeprozeß vermittelt, einen Anionenkanal, dessen physiologische Funktion weniger gut verstanden ist. Bislang wurde angenommen, daß dieser EAAT-assoziierte Anionenkanal den elektrogenen Glutamataufnahmeprozeß unterstützt und die neuronale Erregbarkeit dämpft, indem er das negative Ruhemembranpotential durch eine Erhöhung der Membranleitfähigkeit und eine Verringerung der Membranlängs- und -zeitkonstante stabilisiert.

Zwischen Glutamatcarrier und Anionenkanal, den beiden funktionellen Domänen der EAAT-Transporter, treten Interaktionen auf, die man sich derzeit folgendermaßen vorstellt: Der Kanal kann sich nur in bestimmten Konformationszuständen des Carriers öffnen. In der Abwesenheit von Glutamat bleibt der Kanal geschlossen, da der Carrierzyklus nicht durchlaufen wird. Erst durch die Bindung von Glutamat und Na^+ an den Carrier öffnet sich der Kanal und wechselt während des Carrierzyklus zwischen offenen und geschlossenen Zuständen hin und her. Die Interaktionen zwischen Carrier und Kanal der EAAT-Transporter sind also vergleichbar mit denen zwischen Rezeptor und Pore in ligandengesteuerten Ionenkanälen.

Der carriervermittelte Glutamataufnahmestrom von EAAT4 ist im Vergleich zum kanalvermittelten Anionenstrom vernachlässigbar klein. EAAT4 wird als postsynaptischer Glutamattransporter hauptsächlich in den dendritischen Dornfortsätzen der Purkinje-Neuronen des Kleinhirns exprimiert, die sowohl mit Parallel- als auch mit Kletterfaserendigungen exzitatorische glutamaterge Synapsen bilden. An diesen Synapsen weist der EAAT4 eine perisynaptische Lokalisation auf, das heißt, die höchste Expressionsdichte innerhalb eines Dornfortsatzes findet sich außerhalb des synaptischen Spaltes. Da der EAAT4 für die Glutamataufnahme an diesen Synapsen von untergeordneter Bedeutung zu sein scheint, wird seine Funktion in der Regulation neuronaler Erregbarkeit als glutamatabhängiger Anionenkanal gesehen.

Diskussion

Im Rahmen der vorliegenden Arbeit wurde der EAAT4 heterolog in Säugetierzellinien exprimiert. Diese Zellen eignen sich hervorragend für elektrophysiologische Untersuchungen an Glutamattransportern, da sie vernachlässigbar kleine endogene Anionenstromamplituden aufweisen, die durch Glutamatapplikation nicht beeinflußt werden. In diesem Expressionssystem wurden funktionelle Eigenschaften des EAAT4-assoziierten Anionenkanals mit Hilfe der „patch-clamp"-Technik untersucht. Um rein kanalvermittelte Ströme messen zu können, wurde in der überwiegenden Zahl der Experimente die Carrierfunktion durch Austausch des intrazellulären K^+ gegen Na^+ gehemmt.

Glutamate modifies ion conduction and voltage-dependent gating of excitatory amino acid transporter-associated anion channels, J. Biol. Chem. 2003

Um zu testen, ob das Öffnen des Anionenkanals strikt an die Anwesenheit von Glutamat gebunden ist, haben wir in Anionenaustauschexperimenten überprüft, ob der EAAT4-assoziierte Anionenkanal in Abwesenheit des Carriersubstrates Glutamat eine Leitfähigkeit für Anionen aufweist. Unter allen ionischen Bedingungen sind die gemessenen Ströme signifikant größer als die endogenen Hintergrundströme und nehmen in ihrer Amplitude von Cl^- nach I^-, NO_3^- und SCN^- zu. Aus den Strom-Spannungskennlinien und den gemessenen Umkehrpotentialen unter den verschiedenen ionischen Bedingungen läßt sich eine lyotrope Selektivitäts- und Leitfähigkeitssequenz ($SCN^- > NO_3^- > I^- > Cl^-$) erkennen. Große polyatomische Anionen permeieren die Pore des EAAT4-assoziierten Anionenkanals folglich besser als kleine einatomige. Der EAAT4-assoziierte Anionenkanal weist also auch in Abwesenheit des Carriersubstrates Glutamat eine substantielle, tonische Leitfähigkeit auf. Ferner beobachtet man eine Zunahme des Ausstroms intrazellulärer Cl^--Ionen in Anwesenheit von Anionen höherer Permeabilität auf der extrazellulären Seite der Membran. Dies ist vergleichbar mit einem Transakzelerationsphänomen bei carriervermittelten stöchiometrisch gekoppelten Transportprozessen.

Die Applikation von extrazellulärem Glutamat führt je nach Anionenzusammensetzung zu einer Verdoppelung bis Verdreifachung der „whole-cell"-Stromamplitude. Die Anionenleitfähigkeit in Abwesenheit von Glutamat stellt also einen bedeutenden Teil der Gesamtleitfähigkeit nach vollständiger Aktivierung des Anionenkanals dar. Nach Glutamatapplikation kommt es weiterhin zu einer Verschiebung des Umkehrpotentials. Diese ist weder auf eine Akkumulation oder Depletion von Anionen noch auf die Diffusion von Glutamat durch die Pore des Kanals zurückzuführen. Sie spiegelt vielmehr eine Änderung der relativen Anionenpermeabilität der Kanalpore durch die Bindung von Glutamat an den Carrier wider. Solche Änderungen der Anionenselektivität des Kanals werden auch durch verschiedene Na^+- und K^+-gebundene Zustände des Carriers hervorgerufen.
Die Zunahme des Cl^--Ausstroms in Anwesenheit permeablerer extrazellulärer Anionen sowie die Beeinflussung von Anionenselektivität und -leitfähigkeit der Kanalpore durch verschiedene Konformationszustände des Carriers sind zwei Eigenschaften der EAAT4-assoziierten Anionenleitfähigkeit, die für einen kanalvermittelten Transportprozeß untypisch sind, sich aber bei stöchiometrisch gekoppelten Transportprozessen häufig finden.
Die Untersuchung der Konzentrationsabhängigkeit des Umkehrpotentials unter biionischen Bedingungen ist geeignet, zwischen kanal- und carriervermitteltem Transportmodus zu unterscheiden. Sie tritt nur bei einem nicht gekoppelten, kanalvermittelten Transportprozeß durch eine mehrfach besetzte Pore, das heißt, eine Pore, die mehr als eine Anionenbindungsstelle enthält, auf. Bei Variation der absoluten externen SCN^-- und internen NO_3^--Konzentration und konstantem Verhältnis von externer und interner Anionenkonzentration verschiebt sich das gemessene Umkehrpotential. Der Anionentransport erfolgt also nicht carriervermittelt in einem festen stöchiometrischen Verhältnis, sondern kanalvermittelt durch eine mehrfach besetzte Pore.

Die Anionenströme in Ab- und Anwesenheit von Glutamat zeigen ein spannungs- und zeitabhängiges Aktivierungs- und Deaktivierungsverhalten. Für einen kanalvermittelten Transportprozeß ist die „whole-cell"-Stromamplitude das Produkt der Anzahl der Kanäle in der Membran, der Stromamplitude durch einen einzelnen Kanal und der Offenwahrscheinlichkeit des Kanals. Änderungen der Anzahl der Kanäle in der Membran konnten ausgeschlossen werden. Relaxationen der Stromamplitude können folglich durch Änderungen der Offenwahrscheinlichkeit oder der Einzelkanalstromamplitude bedingt sein. Um zwischen beiden Möglichkeiten zu unterscheiden, wurde eine nicht-stationäre Rauschanalyse in der Abwesenheit von Glutamat unter Verwendung von NO_3^- als extrazellulärem und Cl^- als intrazellulärem Anion durchgeführt. Unter diesen Bedingungen beobachtet man eine besonders deutliche Abnahme der Stromamplitude. Diese zeitabhängige Abnahme der mittleren Stromamplitude ist verbunden mit einer Zunahme der Stromvarianz. Dies belegt eine Änderung der Offenwahrscheinlichkeit während der Stromrelaxationen. Aus der Auftragung der Varianz gegen die mittlere Stromamplitude lassen sich eine Einzelkanalamplitude von 57 ± 7 fA bei +120 mV, entsprechend einer Einzelkanalleitfähig-

keit von etwa 0,5 pS, die Anzahl der Kanäle in der Membran und daraus eine absolute Offenwahrscheinlichkeit von 0,84 ± 0,06 ermitteln. In Abwesenheit des Carriersubstrates Glutamat weist der EAAT4-assoziierte Anionenkanal demnach eine hohe Offenwahrscheinlichkeit bei vergleichsweise kleiner Einzelkanalamplitude auf. Die Verdopplung bis Verdreifachung der „whole-cell"-Stromamplitude durch Glutamat kann daher allein durch eine weitere Zunahme der Offenwahrscheinlichkeit der Anionenkanäle nicht erklärt werden. Offensichtlich kommt es durch Bindung von Glutamat an den Carrier auch zu einer Erhöhung der Einzelkanalstromamplitude des Anionenkanals. Dies steht in Übereinstimmung mit experimentellen Untersuchungen am EAAT2. Nach Glutamatapplikation kommt es hier zur Zunahme der Einzelkanalstromamplitude des Anionenkanals durch selektive Erhöhung der Ratenkonstante für die Anionentranslokation durch die Pore.

Unter Verwendung von NO_3^- als extrazellulärem und Cl^- als intrazellulärem Anion wurde im weiteren das zeit- und spannungsabhängige Schaltverhalten des EAAT4-assoziierten Anionenkanals genauer untersucht. In Abwesenheit von Glutamat deaktivieren die Ströme mit einem biexponentiellen Zeitverlauf mit Zeitkonstanten von etwa 5 und 60 ms. Diese Deaktivierung läßt sich durch eine einfache Boltzmann-Verteilung mit einer minimalen Offenwahrscheinlichkeit von 0,19 ± 0,02 und einer halbmaximalen Deaktivierung bei 75,4 ± 9,2 mV beschreiben. Die Wiederherstellung der Aktivierbarkeit des Kanals nach Deaktivierung erfolgt bei repolarisierten Potentialen und weist einen monoexponentiellen Zeitverlauf mit einer Zeitkonstante von etwa 5 ms auf.
Das Schaltverhalten des EAAT4-Anionenkanals wird modifiziert durch Glutamat. In seiner Anwesenheit deaktivieren die Ströme mit einem monoexponentiellen Zeitverlauf mit einer Zeitkonstante von etwa 5 ms. Die minimale Offenwahrscheinlichkeit erhöht sich auf 0,60 ± 0,05 und die Spannung bei halbmaximaler Deaktivierung auf 106,3 ± 3,2 mV. Weiterhin beschleunigt Glutamat den Prozeß der Wiederherstellung der Aktivierbarkeit nach Deaktivierung, der nun eine Zeitkonstante von etwa 1 ms aufweist. Glutamatbindung an den Carrier führt also zu einer verminderten Deaktivierung des Anionenkanals bei Membrandepolarisation und einer beschleunigten Wiederherstellung der Aktivierbarkeit bei Repolarisation.

Diese Modifikation des Schaltprozesses durch Glutamat, die den Offenzustand des Kanals begünstigt, und die Erhöhung der Anionenstromamplitude duch Zunahme von Offenwahrscheinlichkeit und Einzelkanalamplitude führen zu einer Vergrößerung der EAAT4-Anionenleitfähigkeit. Die resultierende Zunahme der Membrangesamtleitfähigkeit stabilisiert das negative Ruhemembranpotential und dämpft so die neuronale Erregbarkeit.

Die direkte Beeinflussung von Poreneigenschaften wie der Anionenselektivität und der Einzelkanalamplitude des Kanals durch verschiedene Bindungszustände des Carriers deutet

auf eine enge funktionelle Kopplung und große räumliche Nähe von Carrier und Ionenkanal innerhalb des Proteins hin.

A dynamic switch between inhibitory and excitatory currents in a neuronal glutamate transporter, Proc. Natl. Acad. Sci. USA 2005

Der Anionenkanal des EAAT4 weist in Gegenwart von Glutamat nach prolongierter tonischer Membrandepolarisation einen langsamen Schaltprozeß mit Aktivierungs- und Deaktivierungszeitkonstanten im Sekundenbereich („slow gate“) auf. In Gegenwart von Glutamat, nicht aber in seiner Abwesenheit, kommt es nach 3 Sekunden dauernden positiven Vorpulsen zu einer Zunahme der Stromamplitude während eines nachfolgenden kurzen negativen Testpulses. Weiterhin beobachtet man eine zeitabhängige Zunahme der Stromamplitude beim Testpuls nach gradueller Verlängerung der Vorpulsdauer. Bei 10 Sekunden dauernden Testpulsen auf verschiedene negative Potentiale nach einem 3 Sekunden langen aktivierenden Vorpuls kommt es zu einer zeitabhängigen Abnahme der Stromamplitude. Sowohl Zu- als auch Abnahme der Stromamplitude weisen einen monoexponentiellen Zeitverlauf mit Zeitkonstanten im Sekundenbereich auf und spiegeln die Aktivierung und Deaktivierung eines langsamen Schaltprozesses der EAAT4-assoziierten Anionenkanäle wider. Der Zeitverlauf der Deaktivierung ist in Abwesenheit von Glutamat deutlich langsamer als in seiner Anwesenheit. Dieser Schaltprozeß läßt sich auch bei phasischer Membrandepolarisation verschiedener Frequenzen unter einem physiologischen Anionenkonzentrationsgradienten in Gegenwart von intrazellulärem K^+ beobachten und kann daher in vivo in Purkinje-Neuronen auftreten.

Die beobachteten Änderungen der Stromamplitude bei Testpotentialen negativ vom Umkehrpotential sind nicht auf eine intrazelluläre Akkumulation von Anionen während des langen depolarisierenden Vorpulses zurückzuführen. Dies wurde in verschiedenen Experimenten überprüft: Das Verhältnis der Stromamplituden von Vor- und Testpuls sind unabhängig vom EAAT4-Expressionslevel. Die Aktivierung des „slow gates“ erfolgt nur in Anwesenheit von Glutamat. Die Zunahme der Stromamplitude bei negativen Potentialen findet sich auch in „outside-out-patches“, einer Meßkonfiguration, in der akkumulationsbedingte Änderungen von Ionenkonzentrationen aufgrund der kleinen dort auftretenden Ströme nahezu ausgeschlossen sind. „Whole-cell“-Experimente mit dem hClC-Kb Anionenkanal und dessen akzessorischer Untereinheit Barttin im gleichen heterologen Expressionssystem führen während des positiven Vorpulses zu ähnlichen Auswärtsstromamplituden wie in Experimenten mit dem EAAT4, aber zu einer vernachlässigbar kleinen Zunahme der Stromamplitude beim negativen Testpuls. Die Deaktivierung des „slow gates“ bei negativen Testpotentialen ist spannungsabhängig und findet auch statt, wenn die Zelle zwischen den einzelnen kurzen negativen Testpotentialen auf einer Spannung positiv vom Umkehrpotential gehalten wird, bei der es zu einem kontinuierlichen weiteren

Anioneneinstrom in die Zelle kommt. Schliesslich kommt es bei der Deaktivierung des „slow gates“ während bestimmter konstanter Testpotentiale zu einer Richtungsumkehr des Stromflusses von einem anfänglichen Einwärts- zu einem Auswärtsstrom. Diese experimentellen Befunde schließen eine intrazelluläre Akkumulation von Anionen als Ursache der beobachteten Änderungen der Stromamplitude während der Aktivierung des „slow gates“ aus.

Während der Aktivierung des langsamen Schaltprozesses kommt es zu einer Verschiebung des Umkehrpotentials, die den gleichen Zeitverlauf aufweist wie die Zunahme der Stromamplitude beim negativen Testpuls. Dies deutet auf eine Änderung der Selektivität der EAAT4-Anionenkanalpore während des langsamen Schaltprozesses hin. Um genauer zu untersuchen, für welche der anwesenden Ionen sich Änderungen der Permeabilität ergeben, wurde der Zeitverlauf der Verschiebung des Umkehrpotentials bei verschiedenen externen Kationenkonzentrationen gemessen. Änderungen der extrazellulären Konzentration von Na^+ und Ca^{2+} führen zu Änderungen des Umkehrpotentials bei Aktivierung des „slow gates“, während die Umkehrpotentiale bei deaktiviertem „slow gate“ unverändert bleiben. Durch die Aktivierung des „slow gates“ kommt es also zu einer Membranpermeabilität für Na^+- und Ca^{2+}-Ionen. Protonen und Glutamat bleiben dagegen impermeabel. Die aktivierten EAAT4-Kanäle selektieren nicht zwischen verschiedenen monovalenten Kationen, da die gleiche Verschiebung des Umkehrpotentials auftritt, wenn das intrazelluläre Na^+ äquimolar durch K^+ ersetzt wird.
Um relative Kationen-Anionen-Permeabilitätsquotienten mittels der modifizierten Goldman-Hodgkin-Katz Gleichung bestimmen zu können, wurden die Experimente mit NO_3^- als einzigem permeablen Anion auf beiden Seiten der Membran durchgeführt. Bei deaktiviertem „slow gate“ entspricht das gemessene Umkehrpotential dem Nernst-Potential für NO_3^-, das heißt, die EAAT4-Kanäle sind perfekt anionenselektiv. Aus dem „steady-state“-Umkehrpotential nach Aktivierung des „slow gates“ errechnet sich ein $P(Na^+)/P(NO_3^-)$ von 0,14 ± 0,02. Unter der Annahme, daß die relative Anionenpermeabilität durch Aktivierung des „slow gates“ nicht beeinflußt wird, ergeben sich bei Verwendung eines experimentell bestimmten $P(NO_3^-)/P(Cl^-)$ von 9,4 ± 0,4 ein $P(Na^+)/P(Cl^-)$ von 1,3 ± 0,2 und ein $P(Ca^{2+})/P(Cl^-)$ von 1,7 ± 0,2. Geringgradige Änderungen der intrazellulären Anionen-zusammensetzung, die unter diesen experimentellen Bedingungen auftreten, wurden numerisch approximiert und bei der Berechnung der Permeabilitätsquotienten berücksichtigt. Nach dieser Korrektur waren die gemessenen „steady-state“-Umkehrpotentiale unabhängig vom EAAT4-Expressionslevel. Unter physiologischen Bedingungen, unter denen Cl^- das bedeutendste Anion darstellt, weisen EAAT4-assoziierte Kanäle nach Aktivierung des langsamen Schaltprozesses also eine erhebliche Permeabilität für mono- und divalente Kationen auf. Anionen- und Kationenflux erfolgen dabei durch dieselbe Pore, und ein Kationenflux findet nur in Anwesenheit permeabler Anionen statt. Dies spricht für eine

Wechselwirkung zwischen Anionen und Kationen bei der Passage durch die langsam aktivierten EAAT4-Kanäle.

Der langsame Schaltprozeß in EAAT4-Anionenkanälen modifiziert nicht nur die Selektivität der Kanalpore sondern auch ihre Offenwahrscheinlicheit. Um dies experimentell zu zeigen, wurde eine Variante der nicht-stationären Rauschanalyse benutzt: Bei deaktiviertem „slow gate“ und nach partieller Aktivierung wurde die Standardabweichung der Stromfluktuationen bei verschiedenen negativen und positiven Testpotentialen gegen die mittlere Stromamplitude aufgetragen. In solch einer Auftragung ist die Steigung einer linearen Regressionsgeraden ein Maß für die Offenwahrscheinlichkeit des Kanals: Je größer die Offenwahrscheinlichkeit, desto geringer die Steigung. Sowohl im deaktivierten wie im aktivierten Zustand sind die Steigungen für Ströme negativ und positiv vom jeweiligen Umkehrpotential verschieden. Ein- und Auswärtsstrom durch EAAT4-assoziierte Anionenkanäle erfolgen also mit unterschiedlichen Offenwahrscheinlichkeiten. Aktivierung des „slow gates“ führt zu einer selektiven Erhöhung der Offenwahrscheinlichkeit bei Potentialen negativ vom Umkehrpotential, mittlerer Strom und Standardabweichung bei Potentialen positiv vom Umkehrpotential bleiben hingegen gleich. Das „slow gate“ erhöht also nur die Offenwahrscheinlichkeit von Kanälen, die einen Einwärtsstrom, das heißt, einen Influx von Kationen bei gleichzeitigem Efflux von Anionen, vermitteln. Kanäle, die einen Auswärtsstrom vermitteln, bleiben unverändert.

Dieser langsame Schaltvorgang ermöglicht es EAAT4-assoziierten Anionenkanälen, Purkinje-Neuronen entweder zu hemmen oder zu erregen: In Abwesenheit elektrischer Aktivität in den Dendriten der Purkinje-Neuronen sind die EAAT4-assoziierten Kanäle perfekt anionenselektiv und vermindern die neuronale Erregbarkeit. Schnelle Abfolgen von Aktionspotentialen und langsame exzitatorische postsynaptische Potentiale nach repetitiver synaptischer Übertragung aktivieren den langsamen Schaltprozeß und führen zum Auftreten einer Kationenpermeabilität und einer erhöhten Offenwahrscheinlichkeit bei Repolarisation. Dies hat einen erregenden Ionenstrom von einigen Sekunden Dauer und damit eine erneute Depolarisation der dendritischen Dornfortsätze zur Folge.
Aus der Anzahl der EAAT4-Transporter pro Dornfortsatz, die sich in unmittelbarer Nachbarschaft des synaptischen Spaltes befinden und damit nach repetitiver synaptischer Transmission Glutamatkonzentrationen bis zu 1 mM ausgesetzt sind, und dem „slow-gate“-induzierten Einwärtsstrom durch einen einzelnen Kanal beim repolarisierten Membranpotential von etwa -60 mV in Purkinje-Neuronen errechnet sich ein Einwärtsstrom vom etwa 175 pA pro Dornfortsatz. Dieser wird allein durch einen Kationeneinstrom getragen, da das Ruhemembranpotential von ungefähr -60 mV in etwa dem Cl^--Gleichgewichtspotential entpricht. Da die Dornfortsätze von Purkinje-Neuronen einen sehr hohen Eingangswiderstand von etwa 400 MΩ aufweisen, führt ein solcher Einwärtsstrom zu einer Depolarisation der Dornfortsatzmembran von etwa 25 mV. Erst mit zunehmender

Depolarisation tritt ein kompensatorischer Anioneneinstrom auf, der das Membranpotential wieder repolarisiert. EAAT4-assoziierte Anionenkanäle können folglich innerhalb kurzer Zeit und ohne energetisch aufwendige Änderungen von Ionenkonzentrationen zwischen inhibitorischer und exzitatorischer Funktion wechseln und so die Erregbarkeit der Purkinje-Neuronen modifizieren. Aufgrund des Einstroms von Ca^{2+} in den Dornfortsatz bei langsamer Aktivierung der EAAT4-Kanäle, der potentiell weiteres Ca^{2+} aus intrazellulären Speichern freizusetzen vermag, ist ein Einfluß dieser transporter-assoziierten Kanäle auf die neuronale Plastizität in Purkinje-Zellen ebenfalls denkbar.

Zusammenfassung

EAAT-Glutamattransporter besitzen mit dem Glutamatcarrier und dem Anionenkanal zwei miteinander interagierende Funktionsdomänen. Der Carrier des EAAT4 modifiziert neben funktionellen Eigenschaften wie dem Schaltverhalten auch Poreneigenschaften wie die Selektivität und die Einzelkanalleitfähigkeit des Anionenkanals. Eine solche Interaktion zwischen beiden funktionellen Domänen des EAAT4-Proteins liegt wahrscheinlich auch dem spannungsabhängigen langsamen Schaltprozeß in der Gegenwart von Glutamat zugrunde, der Selektivität und Offenwahrscheinlichkeit des Anionenkanals modifiziert. Diese Art der intramolekularen Wechselwirkung zwischen Carrier und Anionenkanal in EAAT-Transportern steht im Gegensatz zu allen bisher bekannten Rezeptor-Poren-Interaktionen in ligandengesteuerten Ionenkanälen.

Lebenslauf

15. Januar 1979	geboren in Georgsmarienhütte als Sohn von Hans-Werner Melzer und seiner Ehefrau Dorothea, geb. Klaas
August 1985 - Juli 1989	Besuch der Grundschule Johannisschule, Wallenhorst
August 1989 - Juli 1991	Besuch der Orientierungsstufe Hollage, Wallenhorst
August 1991- Juli 1998	Besuch des Gymnasiums Carolinum, Osnabrück
Juni 1998	Abitur
August 1998 - September 1999	Zivildienst, DRK Rettungsdienst Landkreis Osnabrück
Oktober 1999 - September 2006	Studium der Humanmedizin an der Rheinisch-Westfälischen Technischen Hochschule Aachen als Stipendiat der Studienstiftung des Deutschen Volkes
November 2001 – März 2005	Promotionsarbeit in der Abteilung Neurophysiologie der Medizinischen Hochschule Hannover und dem Institut für Physiologie der RWTH Aachen (Univ.-Prof. Dr. Ch. Fahlke)
September 2001	Ärztliche Vorprüfung
April 2003	1. Abschnitt der Ärztlichen Prüfung
September 2005	2. Abschnitt der Ärztlichen Prüfung
Oktober 2005 - September 2006	Praktisches Jahr in der Chirurgischen und Medizinischen Universitätsklinik der RWTH Aachen (Chirurgie, Innere Medizin) sowie am Institute of Neurology des University College London (Neurologie)
November 2006	3. Abschnitt der Ärztlichen Prüfung und Approbation
seit Februar 2007	Wissenschaftlicher Assistent, Neurologische Universitätsklinik der Bayerischen Julius-Maximilians-Universität Würzburg (Univ.-Prof. Dr. K. Toyka)

Hannover, den 13.01.2007

Nico Melzer

Erklärung nach § 2 Abs. 2 Nrn. 5 und 6 PromO

Ich erkläre, daß ich die der Medizinischen Hochschule Hannover zur Promotion eingereichte Dissertation mit dem Titel „*Der Anionenkanal des neuronalen Glutamattransporters EAAT4*“ in der Abteilung Neurophysiologie der Medizinischen Hochschule Hannover und dem Institut für Physiologie der RWTH Aachen unter Betreuung von Herrn Professor Dr. Ch. Fahlke ohne sonstige Hilfe durchgeführt und bei der Abfassung der Dissertation keine anderen als die dort aufgeführten Hilfsmittel benutzt habe.

Ich habe diese Dissertation bisher an keiner in- oder ausländischen Hochschule zur Promotion eingereicht.

Weiterhin versichere ich, daß ich den beantragten Titel bisher noch nicht erworben habe.

Ergebnisse der Dissertation wurden in folgenden Publikationsorganen veröffentlicht:

1. Journal of Biological Chemistry, 2003
2. Proceedings of the National Academy of Sciences, 2005

Hannover, den 13.01.2007

Nico Melzer

Danksagung

Herrn Professor Dr. Christoph Fahlke danke ich für die freundliche Überlassung des Themas und die exzellente Betreuung der Arbeit.

Allen Mitgliedern der Arbeitsgruppe am Institut für Physiologie der RWTH Aachen, insbesondere Frau Hannelore Heidtmann und Frau Barbara Poser, danke ich für die Unterstützung und die freundliche Arbeitsatmosphäre.